



**Environmental
Science**
Processes & Impacts

Impact of beaver ponds on biogeochemistry of organic carbon and nitrogen along a fire-impacted stream

| | |
|---------------|---|
| Journal: | <i>Environmental Science: Processes & Impacts</i> |
| Manuscript ID | EM-ART-04-2022-000184.R1 |
| Article Type: | Paper |
| | |

SCHOLARONE™
Manuscripts

Environmental Significance Statement

Beaver populations in North America have been increasing since the early 1900s, as have the occurrence of wildfires in the western U.S., causing beaver ponds to be frequently present within fire impacted watersheds. Thus, it is important to understand how beaver ponds control the retention and transformation of fire-affected organic matter. Here, we analyzed a series of beaver ponds and interconnecting free-flowing streams affected by the 2018 Ryan Fire in Wyoming, USA. We found that fire-impacted organic matter, rich in nitrogen, accumulated within the beaver ponds. We also investigated the microbial communities present in fire-impacted beaver ponds, which has not been previously reported. Our data indicates that beaver ponds function as biogeochemical hotspots controlling downstream water quality within burned watersheds.

Impact of beaver ponds on biogeochemistry of organic carbon and nitrogen along a fire-impacted stream

Holly K. Roth¹, Amelia R. Nelson², Amy M. McKenna^{2,3}, Timothy S. Fegel⁴, Robert B. Young⁵, Charles C. Rhoades⁴, Michael J. Wilkins², Thomas Borch^{1,2*}

¹Department of Chemistry, Colorado State University, Fort Collins, CO, USA

²Department of Soil and Crop Sciences, Colorado State University, Fort Collins, CO, USA

³National High Magnetic Field Laboratory, Ion Cyclotron Resonance Facility, Florida State University, FL, USA

⁴Rocky Mountain Research Station, U.S. Forest Service, Fort Collins, CO, USA

⁵Chemical Analysis & Instrumentation Laboratory, New Mexico State University, Las Cruces, NM, USA

* Corresponding author

Submitted to *ESPI*

April 2022

Keywords

Forest fire, wetland biogeochemistry, organic nitrogen, FT-ICR MS, mass spectrometry, dissolved organic matter, 16S rRNA, metagenomics, UV-Vis Fluorescence, pyrogenic organic matter, pyOM

Abstract

Wildfires, which are increasing in frequency and severity in the western U.S., impact water quality through increases in erosion, and transport of nutrients and metals. Meanwhile, beaver populations have been increasing since the early 1900s, and the ponds they create slow or impound hydrologic and elemental fluxes, increase soil saturation, and have a high potential to transform redox active elements (e.g., carbon, nitrogen, sulfur, and metals). However, it remains unknown how the presence of beaver ponds in burned watersheds may impact retention and transformation of chemical constituents originating in burned uplands (e.g., pyrogenic dissolved organic matter; pyDOM) and the consequences for downstream water quality. Here, we investigate the impact of beaver ponds on the chemical properties and molecular composition of dissolved forms of C and N, and the microbial functional potential encoded within these environments. The chemistry and microbiology of surface water and sediment changed along a stream sequence starting upstream of fire and flowing through multiple beaver ponds and interconnecting stream reaches within a burned high-elevation forest watershed. The relative abundance of N-containing compounds increased in surface water of the burned beaver ponds, which corresponded to lower C/N and O/C, and higher aromaticity as characterized by Fourier transform ion cyclotron resonance mass spectrometry (FT-ICR MS). The resident microbial communities lack the capacity to process such aromatic pyDOM, though genomic analyses demonstrate their potential to metabolize various compounds in the anaerobic sediments of the beaver ponds. Collectively, this work highlights the role of beaver ponds as biological “hotspots” with unique geochemistry and microbiomes in fire-impacted systems.

1. Introduction

Forests provide ecosystem services valued at ~\$5 trillion annually¹⁻³ and are critical global sources of high-quality drinking water.^{4,5} Wetlands contribute to these services, as they filter water, influence biogeochemical cycling, and support local flora and fauna.⁵ Such services are susceptible to natural or anthropogenic disturbances (e.g., wildfire, insect infestation, development, etc.), especially as such disruptions may threaten downstream water quality.⁶ Wildfires are of particular concern in the western U.S., as their frequency, intensity, and duration have increased in recent years and are projected to increase further.^{7,8} This underscores the need to better understand the consequences of severe fire on the ecosystem processes that regulate clean water supply.

Heating and combustion of organic matter during severe wildfires creates pyrogenic organic matter (pyOM),⁹ comprised of char, soot, and condensed polycyclic aromatic molecules and accounts for ~5-15% of soil carbon.¹⁰ The higher hydrophobicity and aromaticity, lower C:N ratios, and longer mean residence times of C in pyOM alters biogeochemical processes compared to unburned soils.¹¹⁻¹³ pyOM may be introduced to fluvial systems in post-fire runoff, which can be enriched in dissolved organic carbon (DOC), nitrogen (N), heavy metals, nutrients, and polycyclic aromatic hydrocarbons.¹⁴⁻¹⁶ Indeed, stream DOC concentrations often increase following fire,¹⁷⁻¹⁹ though its reactivity and impacts on either river microbial communities or water treatment is less certain. Recent studies document elevated post-fire DOC with increased aromaticity and aromatic carboxylic acid concentrations,^{20,21} though a comprehensive molecular-level characterization of these compounds is lacking. Shifts to more recalcitrant functional groups may inhibit microbial metabolism of DOC^{22,23} and preserve pyOM within aquatic ecosystems. Further, exported pyOM from burned catchments is known to have costly short- and long-term impacts on downstream drinking water treatment and aquatic ecosystems.^{6,24} Wildfire effects on water quality can persist for years,¹⁵ and therefore represent important financial and functional challenges for water treatment.¹⁰

Concurrent to increases in fire activity, North American beaver (*castor canadensis*) populations have steadily increased since their near eradication in the northern U.S. in the early 1900s.²⁵ These “ecosystem engineers” build dams and create channels which influence hydrologic and biogeochemical processes with relevance to downstream water quality.^{26,27} The structure of beaver dams and associated physical features are known to influence post-fire stream channel and floodplain geomorphology,³² but their impact on microbial communities and biogeochemical processes remains poorly studied.³⁰ Beaver dams and the floodplain complexity they create trap particulate carbon (C) and nutrients and create reduced zones that are depleted in dissolved oxygen,²⁷ where microbes must rely on alternate electron acceptors for respiration (e.g., NO₃⁻, Fe³⁺).²⁸ Tied to these biogeochemical changes, beaver ponds influence the availability of nutrients, solubility of metals, and quality of C in surface waters and sediments,^{25,29,30} likely affecting C and N dynamics.^{31,32} In contrast to free-flowing stream reaches that favor aerobic respiration, the reducing conditions within beaver ponds favor anaerobic metabolisms. Microbes are known to metabolize pyOM in well-oxygenated soils,^{33,34} but the potential for microbial processing of pyOM under saturated beaver pond anoxic conditions is less well understood. With beaver populations reaching approximately 30 million in North America³⁵ and over 1 million in Eurasia,³⁶ understanding the influence of beaver ponds on pyOM processing is critical to predict C and N cycling in impacted areas.

Nitrogen is a limiting reactant for microbial and plant productivity,^{37,38} and its lability and bioavailability are sensitive to both heating and postfire ecosystem characteristics.^{39,40} Although dissolved nitrogen can remain elevated in streams for years following fire,⁴¹⁻⁴³ little is known about

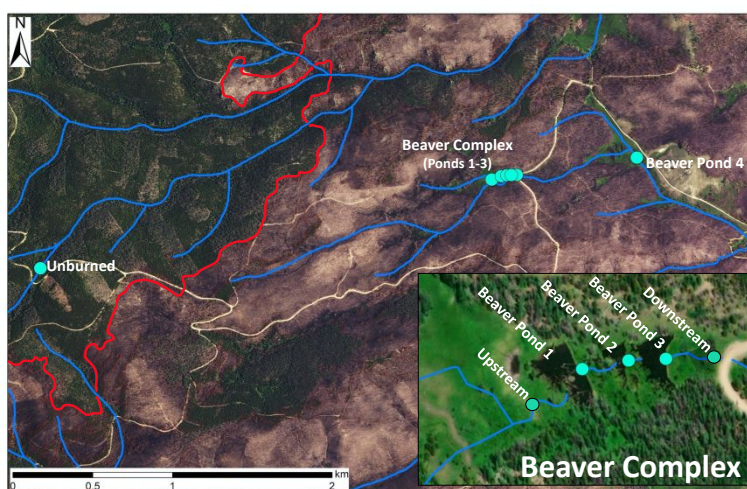
1
2
3 the biotic (e.g., nitrification, dissimilatory nitrate reduction to ammonium) or abiotic (e.g.,
4 sorption, aggregation) processes that regulate soil N cycling and release to surface water.⁴⁴ Fourier
5 transform ion cyclotron resonance mass spectrometry (FT-ICR MS) coupled with electrospray
6 ionization analysis shows that combustion during wildfire creates thermodynamically recalcitrant
7 organic matter that resists microbial degradation and alters C and N cycling.^{45–47} FT-ICR MS
8 permits direct measurement of DON and has shown that the N contained in pyOM is incorporated
9 into refractory, heterocyclic aromatic compounds.^{44,46,48,49} However, molecular transformations
10 which may occur to nitrogenated pyOM in anoxic conditions are not well known, despite the
11 implications they may have for N cycling.^{50,51}

12
13
14 This work investigates potential post-fire changes to surface water C and N chemistry and
15 sediment microbiome composition and function within beaver ponds. Work was conducted in a
16 subalpine forest watershed within the Medicine Bow-Routt National Forest, Wyoming, USA, that
17 burned during the 2018 Ryan Fire. We collected surface water and sediment samples along a series
18 of beaver ponds within a severely burned portion of the watershed (**Fig. 1**). We expected to find
19 higher N concentrations and DOM with higher aromaticity and larger molecular sizes in the beaver
20 ponds compared to free-flowing stream reaches. We hypothesized that changes in surface water
21 molecular speciation would influence microbial communities in beaver pond sediments. Finally,
22 we examined whether microbially mediated biogeochemical processes influence C and N
23 composition or export from fire-affected beaver ponds.
24
25

26 27 2. Methods

28 2.1 Site Description, Sample Collection and Processing

29 Surface water was collected at six locations along a burned stream affected by the 2018
30 Ryan Fire (Middle Fork of Big Creek) starting above a series of four beaver ponds and from an
31 adjacent unburned tributary of McAnulty Creek (**Fig. 1**). Three neighboring ponds were combined
32 and analyzed as a complex, whereas Pond 4 was 3.5 km downstream and was analyzed separately.
33 Surface grab samples (one per sampling location) were collected monthly starting near peak runoff
34 throughout the summer (mid-June through October) one and two years postfire. Stream water
35 samples were collected from the thalweg of the stream and pond samples were collected near the
36 outlet at the sediment-water interface.
37
38
39



1
2
3 **Figure 1:** Sampling locations along Middle Fork of Big Creek within the Ryan
4 Fire near the Colorado-Wyoming border and unburned subalpine forest along a
5 tributary of McAnulty Creek.
6

7
8 Because water chemistry and the environmental microbiome are intimately connected, we
9 used DNA-based methods to characterize the beaver pond microbiome within our sampling sites
10 and adjacent wetlands outside of the Ryan Fire (**Fig. S1**). Based on year 1 observations, we
11 sampled bulk surficial sediments and associated pore water from Beaver Ponds 1, 2, and 4, along
12 with 4 other beaver ponds in adjacent watersheds in the fall of 2020, for a total of seven samples.
13 We additionally attempted to collect only porewater samples from the ponds, but the sediment in
14 the ponds was very fine and all attempts to use porewater “sippers” resulted in them clogging
15 without yielding sufficient sample for analysis. Therefore, surficial sediment and pore water
16 samples (approximately 5 cm depth) were collected from the sediment-water interface using an
17 ethanol-sterilized plastic cup and stored in a cooler for transport. One sediment sample was
18 collected per sampling location.
19
20

21 2.2 Carbon, Nitrogen, and UV-Vis Fluorescence

22 Water samples analyzed for DOC, DTN, and UV-Vis fluorescence spectroscopy were
23 collected in pre-combusted (heated for 3 hours at 500 °C) glass amber bottles and filtered through
24 0.7 µm pore-size glass fiber filters (Millipore Corp, Burlington, MA) within 24 hours of collection.
25 Samples for anion and cation analyses were collected in opaque high-density polyethylene (HDPE)
26 plastic bottles after triple washing with de-ionized water ($EC < 1.0 \mu S\ cm^{-1}$).
27

28 DOC and DTN measurements were performed via high-temperature combustion catalytic
29 oxidation on a Shimadzu TOC-VCPN total organic C/N analyzer with 2 M HCl addition before
30 analysis to remove mineral C (Shimadzu Corporation, Columbia, MD). Inorganic nutrient
31 concentrations were determined by ion chromatography via electrical conductivity detection, using
32 an AS19A Anion-Exchange column for anions and a CS12A Cation-Exchange column for cations
33 (Dionex Corp, Sunnyvale, CA, APHA, 1998a). Detection limits for NO_3^- and NH_4^+ were 10 µg/L.
34 DON is estimated as the difference between DTN and the sum of dissolved inorganic N forms
35 ($NO_3^-N + NH_4^+N$).
36
37

38 Optical parameters, such as fluorescence index (FI), and freshness index (β/α) approximate
39 DOM characteristics, (e.g., aromaticity, degree of microbial processing) to measure shifts in DOM
40 composition.⁵⁰ Although these parameters only reflect the fluorophores in the sample, they can be
41 used to determine variations in DOM source and biogeochemical processes.^{51,52} FI is widely
42 applied in stream water and wildfire studies, as it appears to be particularly sensitive for wildfire-
43 impacted DOM due to increases in oxidized functional groups (increased by ~0.13 in fire-impacted
44 sediment leachates).⁵³ Samples were analyzed using a Horiba Scientific Aqualog (Horiba-Jobin
45 Yvon Scientific Edison, New Jersey, US) with excitation and emission wavelengths from 200-800
46 nm at 3 nm intervals and scan times of 2 seconds. Filtered samples were diluted to 5 mg C/L prior
47 to analysis to reduce inner-filter effects and normalize their concentrations. A sealed cuvette of
48 deionized water was used as a blank and analyzed between every ten samples to correct for
49 instrument drift. The samples were corrected for inner-filter effects and Rayleigh scatter was
50 masked using first and second grating orders after spectral analysis. Finally, each spectrum was
51 normalized by the area of the deionized water Raman scattering peak, as determined by the blank.⁵⁴
52 From this, fluorescence index (FI, Equation 1),⁵⁰ and freshness index were calculated (β/α ,
53 Equation 2).⁵⁵
54
55
56
57
58
59
60

$$FI = \frac{\text{excitation:}370 \text{ nm, emission} \frac{470\text{nm}}{520\text{nm}}}{\text{beta (excitation:}310 \text{ nm, emission } 380 \text{ nm)}} \quad (\text{EQ } 1)$$

$$\beta/\alpha = \frac{\text{alpha(excitation:}310 \text{ nm, emissionmax intensity between } 420 - 435 \text{ nm)}}{\text{beta (excitation:}310 \text{ nm, emission } 380 \text{ nm)}} \quad (\text{EQ } 2)$$

2.4 Fourier Transform Ion Cyclotron Resonance Mass Spectrometry

2.4.1 Sample Preparation

Compositional analysis of the water samples was conducted using FT-ICR MS, used to further explore the differences in DOM composition which cannot be determined by concentration alone. The 21T FT-ICR mass spectrometer achieves high resolving power ($m/\Delta m_{50\%}=2,000,000$ at m/z 200), sub-ppm mass accuracy (20–80 ppb), and high dynamic ranges that allows the assignment of tens of thousands of species per mass spectrum.^{56–58} To increase compositional coverage for basic and acidic species, we applied both positive-ion (+ESI) and negative-ion electrospray ionization (-ESI) to selectively ionize polar species through protonation/deprotonation.^{46,59}

Water samples collected in June 2019 were extracted for FT-ICR MS analysis, with each beaver pond in the beaver complex analyzed separately to evaluate the effect of different retention times on chemical composition. Samples for FT-ICR MS analysis were collected in pre-combusted (heated for 6 hours at 400 °C) glass amber bottles, filtered through 0.2 µm polyether sulfone filters and stored at 4°C to minimize microbial activity. Prior to FT-ICR MS analysis, samples were prepared via solid phase extraction according to Dittmar et al., 2008.⁶¹ Briefly, 500 mL of each sample was acidified to pH 2 using trace metal-grade HCl (Sigma-Aldrich Chemical Co.). Agilent Bond Elut PPL cartridges (3 mL, 200 mg) were prepared by rinsing first with 15 mL methanol followed by 15 mL pH 2 water. PPL cartridges are a common SPE sorbent, as they are selective for many compounds which are prevalent in OM.⁶² PPL selectivity and high extraction efficiency (approximately 40–65% DOC recovery) made them an appropriate sorbent for this analysis.⁶³ Each water sample was passed through a PPL cartridge that was subsequently rinsed with 15 mL pH 2 water to remove salts. Finally, each sample was eluted with 2 mL HPLC grade methanol (Sigma-Aldrich Chemical Co., St. Louis, MO). SPE extracts were ran without further dilution prior to analysis by negative and positive ion electrospray ionization (ESI).⁴⁶

2.4.2 Instrumentation: ESI Source

The sample solution was infused via a micro electrospray source⁶⁴ (50 µm i.d. fused silica emitter) at 500 nL/min by a syringe pump. Typical conditions for negative ion formation were: emitter voltage, -2.7–3.2 kV; S-lens RF (45 %) and heated metal capillary temperature 350 °C. Positive-ion ESI spray conditions were opposite in polarity.

2.4.3 Instrumentation: 21 T FT-ICR MS

SPE extracts were analyzed with a custom-built hybrid linear ion trap FT-ICR mass spectrometer equipped with a 21 T superconducting solenoid magnet.^{58,65} Ions were initially accumulated in an external multipole ion guide (1–5 ms) and released m/z -dependently by decrease of an auxiliary radio frequency potential between the multipole rods and the end-cap electrode.⁶⁶ Ions were excited to m/z dependent radius to maximize the dynamic range and number of observed mass spectral peaks (32–64%),⁶⁶ and excitation and detection were performed on the same pair of electrodes.⁶⁷ The dynamically harmonized ICR cell in the 21 T FT-ICR is operated with 6 V trapping potential.^{66,68} Time-domain transients of 3.1 seconds were acquired with the Predator data station that handled excitation and detection only, initiated by a TTL trigger from the commercial Thermo data station, with 100 time-domain acquisitions conditionally-coadded for

all experiments.⁶⁹ Mass spectra were phase-corrected⁷⁰ and internally calibrated with 10-15 highly abundant homologous series that span the entire molecular weight distribution based on the “walking” calibration method.⁷¹ Mass spectral peaks with signal magnitude greater than six-times the baseline root-mean-square noise level at m/z 500 were exported to a peak list. Experimentally measured masses were converted from the International Union of Pure and Applied Chemistry (IUPAC) mass scale to the Kendrick mass scale⁷² for rapid identification of homologous series for each heteroatom class (i.e., species with the same $C_cH_hN_nO_oS_s$ content, differing only by degree of alkylation).⁷³ For each elemental composition, $C_cH_hN_nO_oS_s$, heteroatom class, double bond equivalents (DBE = number of rings plus double bonds to C, $DBE = C - h/2 + n/2 + 1$)⁷⁴ and C number, c , were tabulated for subsequent generation of heteroatom class relative abundance distributions and graphical relative-abundance weighted images and van Krevelen diagrams. Molecular formula assignments and data visualization were performed with PetroOrg © software.⁷⁵ Molecular formula assignments with an error >0.25 parts-per-million were discarded, and only chemical classes with a combined relative abundance of $\geq 0.15\%$ of the total were considered. All FT-ICR MS spectra are publicly available through the Open Science Framework (<https://osf.io/t4eqx/>) (DOI 10.17605/OSF.IO/T4EQX).

2.4.4 Molecular Formula Calculations

Assigned elemental compositions from neutral species were used to calculate O/C and C/N ratios, modified aromaticity index (AI_{mod} ; Equation 3),^{76,77} and nominal oxidation state of carbon (NOSC; Equation 4).⁷⁸ Van Krevelen diagrams were also constructed from the FT-ICR MS results, in which the elemental ratio of O/C is plotted on the x-axis and the H/C ratio is plotted on the y-axis to visualize the spread of the assigned formulas and major compositional shifts.⁷⁹

$$AI_{mod} = \frac{1 + C - \frac{1}{2}O - S - \frac{1}{2}(N + P + H)}{C - \frac{1}{2}O - N - S - P} \quad (\text{EQ 3})$$

$$NOSC = 4 - \frac{4C + H - 2O - 3N - 2S}{C} \quad (\text{EQ 4})$$

C = carbon, H = hydrogen, O = oxygen, N = nitrogen, S = sulfur, P = phosphorus

2.5 Microbial Analyses

2.5.1 DNA extraction and 16S rRNA gene sequencing

To extract pore fluids and corresponding microbial communities, sediment-pore water slurries were centrifuged at 7000 rpm for 10 minutes and the supernatant was then pulled off and filtered through a 0.22 μm filter. DNA was extracted from the filters using the Zymobiomics Quick-DNA Fecal Soil Microbe Kits (Zymo Research, Ca, USA). For community composition analysis, 16S rRNA genes in the extracted DNA were amplified and sequenced at Argonne National Laboratory (primer set 515F/806R). Raw sequencing data was processed using the QIIME2 pipeline (QIIME2-2019.10), reads were clustered into amplicon sequence variant (ASV) classifications at 99% similarities, and taxonomy was assigned using the QIIME2 scikit-learn classifier trained on the SILVA⁸⁰ (release 132) database.⁸¹ All 16S rRNA gene sequencing data is available at NCBI and can be accessed under accession number PRJNA792827. Mean species diversity of each sample (alpha diversity) was calculated based on species abundance and evenness using Shannon’s Diversity Index (H), Pielou’s Evenness (J), and species richness (R vegan package).

2.5.2 Metagenomic sequencing and binning

A subset of seven beaver pond sediment samples were selected for metagenomic sequencing to analyze metabolic functional potential within these sediments. Three of these samples were recovered from BP1, 2, and 4, while four other samples were collected from additional beaver wetlands outside the Ryan Fire burn scar (**Fig. S1**). Libraries were prepared using the Tecan Ovation Ultralow System V2 and were sequenced on the NovaSEQ6000 platform on a S4 flow cell at Genomics Shared Resource, Colorado Cancer Center, Denver, CO, USA. Sequencing adapters were removed from reads using Bbduk (<https://jgi.doe.gov/data-and-tools/bbtools/bb-tools-user-guide/bbduk-guide/>), and Sickle (v1.33)⁸² was used to trim reads. FastQC (v0.11.2) was used before and after trimming reads to ensure high-quality reads were used for downstream processing. Trimmed metagenomic reads are available on NCBI and can be accessed under accession number PRJNA792827. Reads were assembled into contiguous sequences (contigs) using MEGAHIT (v1.2.9)⁸³ with a minimum kmer of 27, maximum kmer of 127, and step of 10 bp. Assembled contigs greater than 2500 bp were binned using Metabat with default parameters (v2.12.1).⁸⁴ We additionally used co-assembly techniques to maximize the number of bins from this dataset. The final metagenome-assembled genomes (MAGs) were assessed for completion and contamination using checkM v1.1.2⁸⁵ and taxonomy was assigned using GTDB-Tk v1.3.0.⁸⁶ The final MAG dataset was combined and dereplicated using dRep v3.0.0⁸⁷ to create the complete non-redundant database. MAG relative abundance across each sample was calculated using coverM genome v0.6.0 (<https://github.com/wwood/CoverM>). All quality metrics and taxonomy for the 33 medium- and high-quality MAGs discussed here are included in the supplementary material (**Supplementary Data 1**) and are deposited on Zenodo (DOI: 10.5281/zenodo.5806541). MAGs were annotated using DRAM v1.2.⁸⁸ To identify multiheme c-type cytochromes (MHCs), we used the Geneious Prime (version 2020.0.3) ‘Search for motifs’ tool to identify protein sequences with at least 3 CXXCH motifs. To remove MHCs not involved with metal reduction, we used the DRAM annotations to remove any sequences annotated as a function likely unassociated with metals. We then analyzed these sequences using PSORTb (v3.0.2)⁸⁹ to remove any proteins that were predicted to remain within the cytoplasm.

2.6 Statistical Analyses

DOC, DTN, %DON, and C:N were evaluated for statistical significance using student’s t-test. All burned samples were compared to the unburned sample for these analyses. First, an F test was performed to assess the equality of variances between samples. If $F_{\text{calculated}}$ (Equations 5&6) is greater than F Critical one-tail (determined by degrees of freedom), the difference in variability between measurements is significant, and the variances are unequal; a lower $F_{\text{calculated}}$ indicates equal variances.⁹⁰ The results of the F test were used to inform the appropriate t-Test (Two-Sample Assuming Equal or Unequal Variances) to determine if the difference in sample means was significant. If t Stat (Equations 7&8) is less than t Critical two-tail (determined by degrees of freedom at 95% confidence interval), the difference is not significant; a higher t Stat indicates a significant difference.⁹⁰ A significance level of 0.05 was used for statistical significance in all analyses, and all results are reported in **Table S2**.

$$F_{\text{calculated}} = \frac{s_1^2}{s_2^2} \quad (\text{EQ 5})$$

$$\text{Where } s = \sqrt{\frac{\sum_i (x_i - x_{\text{avg}})^2}{n - 1}} \quad (\text{EQ 6})$$

$$t = \frac{|x_{1\text{avg}} - x_{2\text{avg}}|}{s_{\text{pooled}}} \sqrt{\frac{n_1 n_2}{n_1 + n_2}} \quad (\text{EQ 7})$$

$$\text{Where } S_{\text{pooled}} = \sqrt{\frac{s_1^2(n_1 - 1) + s_2^2(n_2 - 1)}{n_1 + n_2 - 2}} \quad (\text{EQ 8})$$

2.7 Iron Analyses

Water samples for ICP-MS were filtered through ashless Whatman paper filters (GE Healthcare) and acidified to 2% HNO₃ prior to analysis. Elemental concentrations of iron (Fe) were measured via a NexION 250D mass spectrometer (PerkinElmer, Waltham, MA) connected to a PFA-ST nebulizer (Elemental Scientific, Omaha, Nebraska) and Peltier controlled (PC3x, Elemental Scientific) quartz cyclonic spray chamber (Elemental Scientific) set at 4°C. Samples were introduced using a prepFAST SC-2 autosampler (Elemental Scientific). The nebulizer gas flow was optimized for maximum Indium signal intensity (58380 counts per second, 0.82 L/min). To minimize interferences, these measurements were made in dynamic reaction cell mode using ammonia as the reactive gas. Iron (Fe) concentrations reported represent the sum of the detected concentrations of ⁵⁴Fe and ⁵⁶Fe. The detection limits for ⁵⁴Fe and ⁵⁶Fe were 7.24 and 6.46 ppb, respectively.

3. Results and Discussion

3.1 DOC and DTN increase within beaver ponds

DOC concentrations in the surface grab samples throughout the fire-impacted stream varied on both spatial (**Fig. 2a**) and temporal scales (**Fig. S2**). Average DOC concentrations were highest in June 2019 (6.42 ppm, one year after fire, immediately following snow melt) and decreased from June to October (averaging 6.42 ppm to 3.60 ppm, respectively). Such seasonal changes to DOC concentrations have been documented in other high-elevation ecosystems⁹¹ as well as in fire-impacted streams.¹⁵ While DTN averages also varied throughout the summer, the highest average was reported in August 2019 (0.33 ppm) and the lowest in October (0.21 ppm). Seasonal variations in N export agree with changes observed following the 2012 Hayman Fire in Colorado, in which DTN export varied by month.¹⁵

There was no difference in DOC concentrations between the unburned stream and the burned stream above the beaver ponds (**Fig. 2a**). DOC roughly doubled and increased steadily as water passed through the sequence of beaver ponds; however, this difference was not significant (**Table S2**). Average DTN exhibited a similar trend; the unburned and upstream sites were roughly the same concentrations, and the concentrations in beaver ponds were nearly twice those of the sites preceding them (**Table S1**). In contrast with DOC, DTN increases within the ponds were statistically significant (**Table S2**). Importantly, the beaver ponds typically contained higher concentrations of DOC and DTN than the site upstream of them (**Fig. 2b**), in agreement with previous studies conducted on beaver ponds which have shown that these features influence organic C storage by trapping large quantities of sediment and organic material,^{92,93} therefore affecting C and N dynamics within those sites.³¹ Further evidence of a shift in C and N dynamics is provided by the C:N ratio, which was 32 in the unburned stream and fluctuated between 16-20 in the burned stream (**Table S1**). While these differences are not significant (**Table S2**), they do represent a shift =below the commonly accepted threshold in which microbes are no longer N limited (C:N ratio of 24).⁹⁴

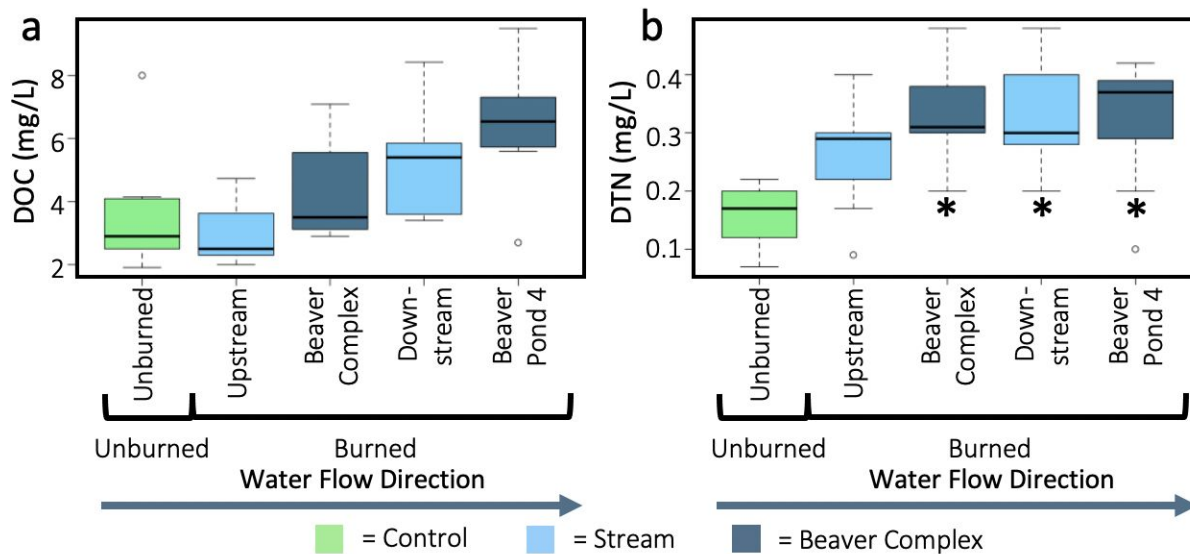


Fig. 2: Dissolved organic carbon (DOC, left) and dissolved total nitrogen (DTN, right) concentrations along a stream impacted by the 2018 Ryan fire and an adjacent unburned stream (**Fig S1**). The lower and upper hinges of the boxplots represent the 25th and 75th percentile and the middle line is the median. The upper whisker extends to the median plus 1.5x interquartile range and the lower whisker extends to the median minus 1.5x interquartile range and are comprised of the data from five months of sampling one-year post-fire. Outliers are identified by open circles, and asterisks identify statistical significance.

DON constitutes a large percentage of DTN in unburned free-flowing rivers (62-99%).⁴⁴ Soil and stream nitrate commonly increase following fire due to decrease of plant uptake, leaching losses and increased nitrification.^{95,96} Stream nitrate and DTN were both elevated in watersheds affected by extensive, severe wildfire in ponderosa pine forests in Colorado, but increases in nitrate caused the fraction of DTN comprised by DON to decline from 35% in unburned catchments to 6% in burned catchments.¹⁵ Both nitrate and DTN roughly doubled within the Ryan fire, which indicates minimal wildfire effect on the proportion of DTN comprised by DON. Nitrate declined by about 40% downstream of the Beaver Complex, consistent with denitrification in the anoxic beaver pond soils (**Fig. S3**). Nitrate decline resulted in substantial increases in %DON within the ponds, constituting 60% of DTN in the Beaver Complex and 75% of DTN in BP4 (**Table S1**). Although increases in ammonium (NH_4^+) concentrations in rivers following fires have been reported, they were primarily attributed to stormwater events⁴², which were not included in this study. NH_4^+ concentrations we report showed no appreciable changes on a spatial or temporal scale, remaining very low across the entire sampling gradient, often below 0.01 ppm (**Fig. S4**). While only our DTN values were statistically significant (**Table S2**), this value supports our hypothesis that total N would be enriched within the beaver ponds, resulting in an increased concentration of DTN and higher %DON in comparison to the unburned and upstream sites (**Table S1**). Local changes in DOC and DTN trends through the stream and beaver ponds may indicate that the influx of pyDOM, among other watershed-derived inputs, into anoxic waters may be less favorable for microbial respiration,⁹⁷ leading to localized increases in %DON.

3.2 Nitrogen-containing compounds are enriched within beaver ponds

The elemental class distribution of the surface grab samples for both ionization modes is listed in **Fig. 3** (formula counts) and **Table 1** (% relative abundances). Within the -ESI spectra, there is an overall decrease in the %CHO and increase in %CHNO between the burned and unburned stream (**Table 1**), although the CHO fraction still constitutes most formulas assigned (6,922 to 9,065 formulas and represents 82.2-89.7% of the spectrum). The smallest number of CHO formulas and lowest %CHO were assigned for Beaver Pond 1 (BP1), accompanied by an increase in %CHNO at the site, consistent with the observed increase in DTN in that pond (**Fig. 2**). The other beaver ponds (BP2, BP3, BP4) also display fewer CHO formulas than the non-beaver pond sites (Unburned, Upstream, Downstream). CHNO variability through the stream resulted in the lowest number of formulas assigned for BP2 (**Fig. 3**). Importantly, this site also has lower DTN concentrations and a lower %DON than the other beaver ponds (**Table S1**). Contrary to other wetland studies, calculated O/C ratios do not appear to be substantially affected by the presence of beaver ponds. Within the sites analyzed here, assigned O/C ratios varied by 0.03 throughout the entire stream (**Table S3**), a magnitude of change smaller than that observed in Florida wetlands, where O/C increased by ~ 0.2 .⁴⁵ Thus, the observed changes in O/C ratios at the Ryan Fire site are likely not large enough to fundamentally alter the ability of the microbial community to process the pyDOM inputs. To further investigate this, we calculated the nominal oxidative state of carbon (NOSC), which describes a molecule's lability through its direct relationship to the Gibbs free energy (ΔG°) of the reduction half-reaction between organic matter (electron donor) and a terminal electron acceptor (e.g., O_2 , NO_3^- , Fe^{3+} , SO_4^{2-}) (**EQ S1**).⁷⁸ NOSC values showed little variation between sampling locations and remained above the thermodynamic limits for standard state ($NOSC < -0.6$) and sulfidic reduction ($NOSC < -0.3$)⁹⁷ (**Table S3**), indicating that thermodynamic limitations associated with oxygen and sulfate reduction (representing the highest and lowest energy yields, respectively) do not apply with respect to NOSC in these samples. Therefore, compositional changes identified through FT-ICR MS are likely not a limiting factor for microbial respiration. However, it is important to note that this value can only be used to predict whether respiration is thermodynamically favorable, and not whether a microbial community is actively transcribing the genes necessary for the breakdown of these compounds.

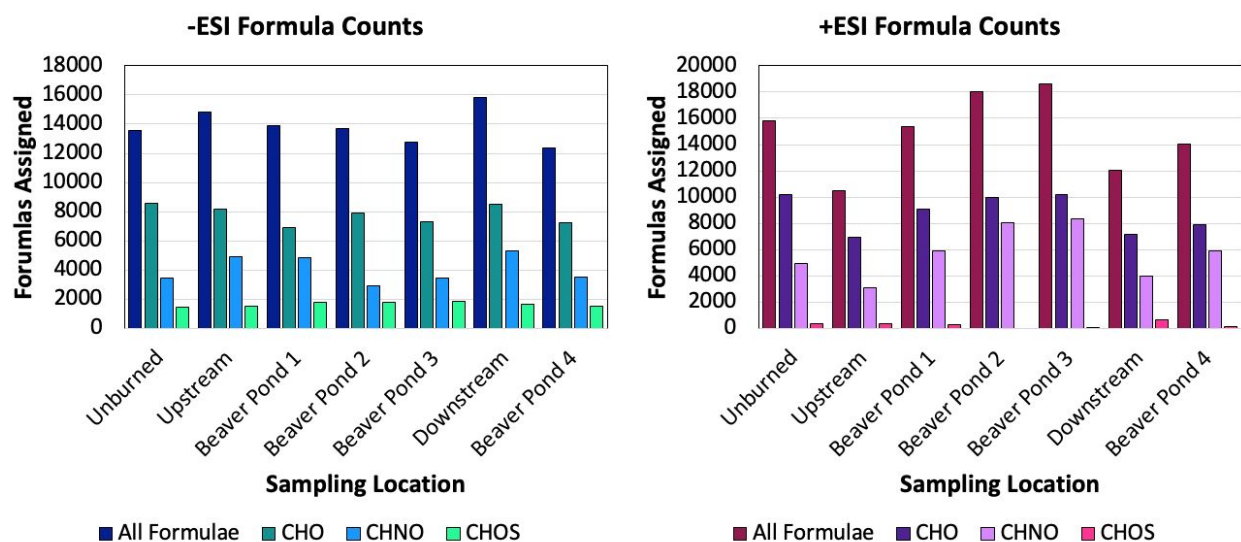


Fig. 3: Elemental composition assignments derived from +/- ESI FT-ICR MS at 21 T mass spectra for the Ryan Fire PPL water extracts. Bar charts include the assigned formula counts for each heteroatom class assigned. -ESI bar chart on the left and +ESI bar chart on the right. C = carbon, H = hydrogen, N = nitrogen, O = oxygen, S = sulfur.

Table 1: FT-ICR MS data collected via electrospray ionization in negative and positive mode for the Ryan Fire water PPL extracts. % abundance data for -ESI reported on top, +ESI results on the bottom. Sampling locations located within the burned area are highlighted in grey.

| ESI Negative Mode | Unburned | Up-stream | Beaver Pond 1 | Beaver Pond 2 | Beaver Pond 3 | Down-stream | Beaver Pond 4 |
|-------------------|----------|-----------|---------------|---------------|---------------|-------------|---------------|
| CHO | 89.7 | 84.8 | 82.2 | 84.6 | 84.7 | 84.2 | 86 |
| CHNO | 6.41 | 10.3 | 11.7 | 10.3 | 9.5 | 11.3 | 9.55 |
| CHOS | 3.74 | 4.69 | 5.75 | 4.95 | 5.68 | 4.09 | 4.39 |
| ESI Positive Mode | Unburned | Up-stream | Beaver Pond 1 | Beaver Pond 2 | Beaver Pond 3 | Down-stream | Beaver Pond 4 |
| CHO | 84.6 | 78.8 | 75.7 | 70.6 | 68.9 | 66.4 | 70.9 |
| CHNO | 14.8 | 9.72 | 17.5 | 29.4 | 30.5 | 14.2 | 26.9 |
| CHOS | 0.385 | 11.1 | 6.61 | 0 | 0.612 | 18.7 | 2.09 |

Complementary +ESI data also displays class element variability throughout the stream (**Table 1**). The site with the least CHO formulas assigned was Upstream, while the site with the lowest %CHO (66.4%) was Downstream. %CHO steadily declined through each of the successive ponds (BP1, BP2, BP3). This was accompanied by changes in the CHNO fraction, which increased from 3,069 formulas Upstream to 8,336 in BP 3 (**Fig. 3**), accompanied by substantial increases in %CHNO. In general, both positive and negative ESI displayed an increase in the number of nitrogenated formulas assigned within the beaver ponds, in conjunction with the increased %DON within those sites (**Table S1**). Here, we report more N-containing compounds (**Table 1**), lower C/N ratios, and higher average N per formula assigned within the beaver ponds compared to the free-flowing sites (**Table S4**), evidence for a shift in DOM processing. Previous studies have observed that heterocyclic N-compounds and aromatic N structures are formed and enriched during the heating of soil OM and plant biomass⁹⁸⁻¹⁰¹ that may describe the CHNO species we detected within the beaver ponds. We compared the tens of thousands of individual elemental compositions identified by FT-ICR MS with van Krevelen diagrams to visualize major shifts in the molecular composition and biological precursor.^{56,79,102} For each plot, the mass spectrum was compared to the unburned control, and we subtracted all common formulas between the two spectra. We further refined our analysis to only those formulas that contained N, using only the +ESI data as this method has been demonstrated to increase the compositional coverage of CHNO species compared to -ESI.⁴⁶ We present van Krevelen diagrams that display only these unique nitrogenated species (unburned control = green markers, burned site = blue markers) (**Fig. 4**), which show that CHNO type and quantity differs as the water travels through the stream. Upstream (**Fig. 4a**), the unique CHNO is centered in the mid-aromatic region. Through the beaver complex, unique CHNO increases in number and expands within the van Krevelen diagram space, first in the aromatic region in BP1 (**Fig. 4b**), and later covering both the aromatic and aliphatic regions of the van Krevelen diagram (**Fig. 4b-d, f**). This expansion mirrors the observed increase in in DTN

and %DON (**Table S1**) and indicates that there is regional preservation of CHNO compounds within these ponds, likely due to lower oxygen levels which in turn promote anaerobic metabolism within the microbial community. Indeed, microbial analyses indicate a diversity of putative anaerobic metabolisms within these locations (**Fig. 6**). Downstream of BP3 the unique CHNO rapidly decreases (**Fig. 4e**) before increasing again in BP4 (**Fig. 4f**), further indicating that CHNO type and quantity is heavily reliant on its environment and its preservation is indeed highly localized.

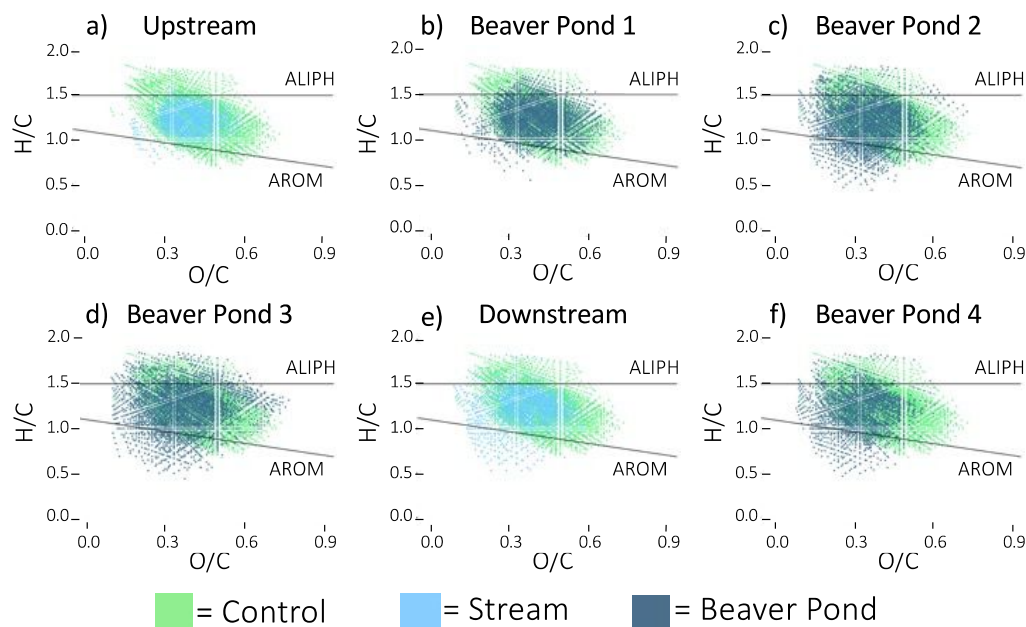


Fig. 4: van Krevelen diagrams plotting the H/C and O/C ratios of the N-containing fraction (i.e., CHNO) obtained via +ESI FT-ICR MS of Ryan Fire stream and beaver pond PPL extracts of the unburned control (green) and burned sampling site (blue, see plot title for specific site). Darker blue denotes beaver ponds. Formulas in common are subtracted out, so that only the formulas unique to each sample are plotted. Formulas plotted below the line that intercepts at H/C 1.2 are generally more aromatic in nature, while those plotting above the line that intercepts at 1.5 are more aliphatic.⁷⁶

3.3 FI and β/α are influenced by fire and wetland presence

FI is commonly used to infer the source of OM (i.e., microbial or terrestrial), where FI = 1.8 indicates microbially-derived DOM and FI = 1.2 indicates terrestrially derived.¹⁰³ While this does not directly measure fire inputs, shifts in FI may represent important differences in microbial processing requirements. We observed an increase in FI values in the surface grab samples through the burned portion of the stream (**Fig. S5**) which indicates that fire-influenced DOM more closely resembles microbially-derived DOM, in agreement with previous studies,⁵³ and is consistent with decreased molecular weight (MW) during the combustion of DOM.¹⁰⁴ This is supported by FT-ICR MS data which indicated that beaver ponds had lower average MW than free-flowing streams (**Table S4**). While our FI values for the beaver ponds fall within previously reported ranges for wetlands (approx. 1.3-1.5),⁹² there was no appreciable difference between the beaver ponds and the Upstream or Downstream sampling location.

1
2
3
4
5
6
7
8
9
10
11
12
13
14
15
16
17
18
19
20
21
22
23
24
25
26
27
28
29
30
31
32
33
34
35
36
37
38
39
40
41
42
43
44
45
46
47
48
49
50
51
52
53
54
55
56
57
58
59
60

Additionally, β/α is used to infer the proportion of recently produced DOM, in which the beta peak represents recently produced (likely microbial) DOM and the alpha peak represents older, more decomposed DOM.¹⁰⁵ β/α follows a similar trend to FI, increasing with burn activity and remaining elevated throughout the beaver ponds (**Fig. S6**). Increases in β/α have been reported following fire¹⁰⁶ and within wetlands,⁹² attributed to more simple structures with lower molecular weight and lower dissolved oxygen, respectively.

3.4 Microbial communities drive diverse anaerobic metabolisms in beaver ponds

Fire can have indirect effects on wetland microbes through broad changes in geochemistry (e.g., C, N availability). A combination of marker gene (16S rRNA gene) and metagenomic sequencing was used to investigate how the observed changes in aqueous chemistry impacted the microbiomes associated with the beaver pond sediments. 16S rRNA gene sequencing of sediment samples showed that the microbial communities within BP1, 2, and 4 were dominated by the phylum *Proteobacteria* (average relative abundance of ~35%; **Fig. 5a**). Within the *Proteobacteria*, the class *Deltaproteobacteria*, which is widely known for anaerobic metabolisms^{107,108} and is frequently identified as one of the most common taxa in wetlands,¹⁰⁹ was the most prevalent throughout the complexes (~20% average relative abundance). Notable orders within the *Deltaproteobacteria* included *Desulfomonadales*, *Syntrophobacterales*, and *Desulfobacterales* (average relative abundances of 4.4%, 6.5%, and 2%, respectively; **Fig. 5b**), which include known sulfate reducers and are therefore well-suited for low-oxygen environments, such as beaver ponds.¹¹⁰

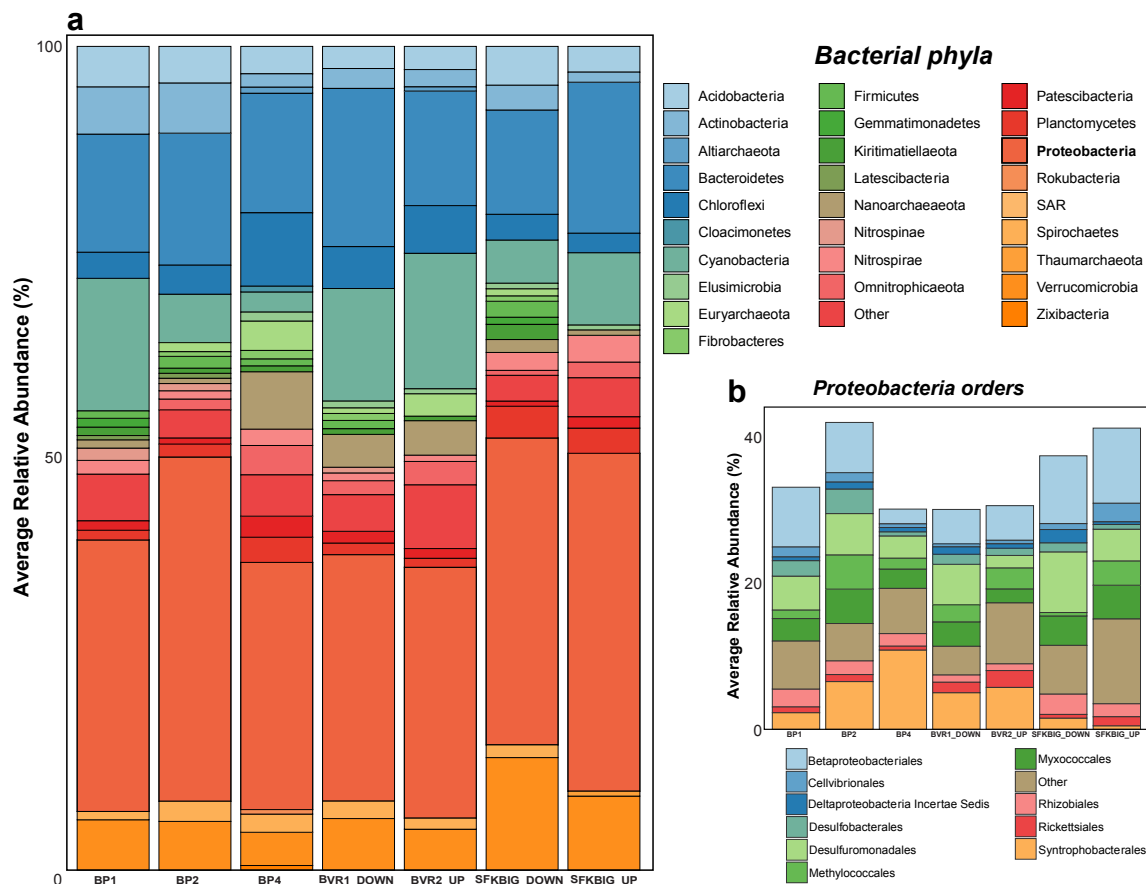


Fig. 5: (a) Bacterial community composition (from 16S rRNA gene sequencing) showing bacterial phyla from beaver pond sediment samples affected by the Ryan fire (BP1, 2, 4) and adjacent control beaver ponds (BVR1_DOWN, BVR2_UP, SFKBIG_UP, SFKBIG_DOWN) shown with the relative abundance of dominant bacterial phyla. Community composition is generally consistent across sample sites. (b) The relative abundance of orders within the dominant bacterial phyla, *Proteobacteria*, across samples. For both A and B, all phyla and orders with average relative abundance <0.005 (0.5%) added to ‘Other’.

The microbial communities observed within the Ryan Fire beaver ponds were consistent across additional beaver ponds burned by the Beaver Creek Fire. These nearby wetlands were also dominated by *Deltaproteobacteria* (~15% average relative abundance) and *Desulfuromonadales*, *Syntrophobacterales*, and *Desulfobacterales* orders (4.4%, 3.2% and 1.5% respectively) (Fig. 5), indicating that fresh pyDOM input did not significantly impact the dominant phyla within the beaver ponds. However, the more recently burned beaver pond microbiome was more compositionally diverse than nearby burned soils. Average species richness (number of unique microbial taxa in a sample) within the beaver complexes was approximately double that in nearby burned soils (995 and 503 total species, respectively),³⁴ likely explained by a combination of factors including significant reductions in soil microbial diversity driven by wildfire events^{111,112}

1
2
3 and increased DOC and DON complexity within the ponds driven by possible pyDOM
4 inputs.^{111,112}

5 From the metagenomic sequencing of the seven sediment samples, including BP1, 2, and
6 4, we reconstructed 33 medium and high-quality (>50% complete, <10% contaminated)¹¹³
7 metagenome-assembled genomes (MAGs), representing the majority of the dominant community
8 members in the corresponding 16S rRNA gene dataset. The MAGs encompassed 12 different
9 phyla, including 14 MAGs from the *Desulfobacterota*, 7 from the *Proteobacteria*, and 3 from the
10 *Acidobacteria*. We linked *Deltaproteobacteria* amplicon sequence variants (ASVs) with two
11 *Desulfobacterota* MAGs (with BLAST matches between 16S rRNA gene ASVs and MAG contigs
12 containing 16S rRNA genes of > 95% identity over at least 150 bp). We infer that due to known
13 taxonomic inconsistencies between the SILVA and GTDB-TK databases, MAGs classified as
14 *Desulfobacterota* are taxonomically equivalent to the *Deltaproteobacteria* ASVs. The
15 *Desulfobacterota* taxa was dominant in the MAG dataset, accounting for 14 of the 33 MAGs and
16 ~35% of the relative abundance across the three main samples.
17

18
19 Highlighting the distinct chemical conditions found within beaver ponds, we identified a
20 range of putative microbial metabolisms that, in contrast, are generally not observed in fire-
21 impacted soils.³⁴ We inferred a fermentative lifestyle for several MAGs (i.e., A_BP_metabat.1,
22 All_co_assemble_metabat.86) that encoded a diverse suite of carbohydrate-active enzymes
23 (CAZymes) (**Fig. S7**), but which lacked a complete TCA cycle and electron transport chain
24 components (e.g., NADH dehydrogenase, cytochrome C oxidase) (**Fig. 6a**). Furthermore, these
25 MAGs likely yield fermentation waste products (e.g., short-chain fatty acids) that can be utilized
26 as both C and electron sources by many of the other MAGs (e.g., *Desulfobacterota*) that perform
27 respiratory metabolisms (**Fig. 6d**). Indeed, the 14 *Desulfobacterota* MAGs encoded widespread
28 genomic potential for anaerobic respiratory metabolisms, including metal reduction (i.e., Fe³⁺,
29 Mn⁴⁺), which could drive increased aqueous metal concentrations in the beaver complexes (**Fig.**
30 **S8**), and potentially cause the observed increases in DOC and DON in the beaver ponds (**Fig. 2**)
31 and the increased number of formulas assigned in the +ESI spectra (**Fig. 4**) through the dissolution
32 of DOM-metal complexes.¹¹⁴ This functionality was inferred from the presence of genes encoding
33 multi-heme c-type cytochromes (MHCs), which are used to transfer electrons to extracellular
34 electron acceptors¹¹⁵ Of the 33 recovered MAGs, 29 encoded MHCs, including all 14 of the
35 *Desulfobacterota* MAGs (**Fig. 6c**). Eleven of these 14 MAGs had MHCs that could be localized
36 to the periplasm or extracellular space (average of 31 cytochromes per MAG; **Fig. 6c**), with an
37 average of ~7 CXXCH motifs per cytochrome (range of 3-16), which is similar to iron reducing
38 microorganisms in other systems.¹⁰⁸ Another prevalent anaerobic metabolism is sulfate reduction,
39 identified here through the presence of reductive *dsrAB* genes. Fourteen MAGs – including 10
40 *Desulfobacterota* MAGs – encoded these enzymes, further revealing the capacity for diverse
41 metabolisms within the beaver ponds (**Fig. 5c**). Importantly, our calculated NOSC values indicate
42 that the DOM in the beaver ponds is not energetically constrained from reduction by these alternate
43 electron acceptors (**Table S3**)⁹⁷ and is a suitable substrate for the wide range of metabolisms
44 identified in the ponds.
45
46
47
48
49
50
51
52
53
54
55
56
57
58
59
60

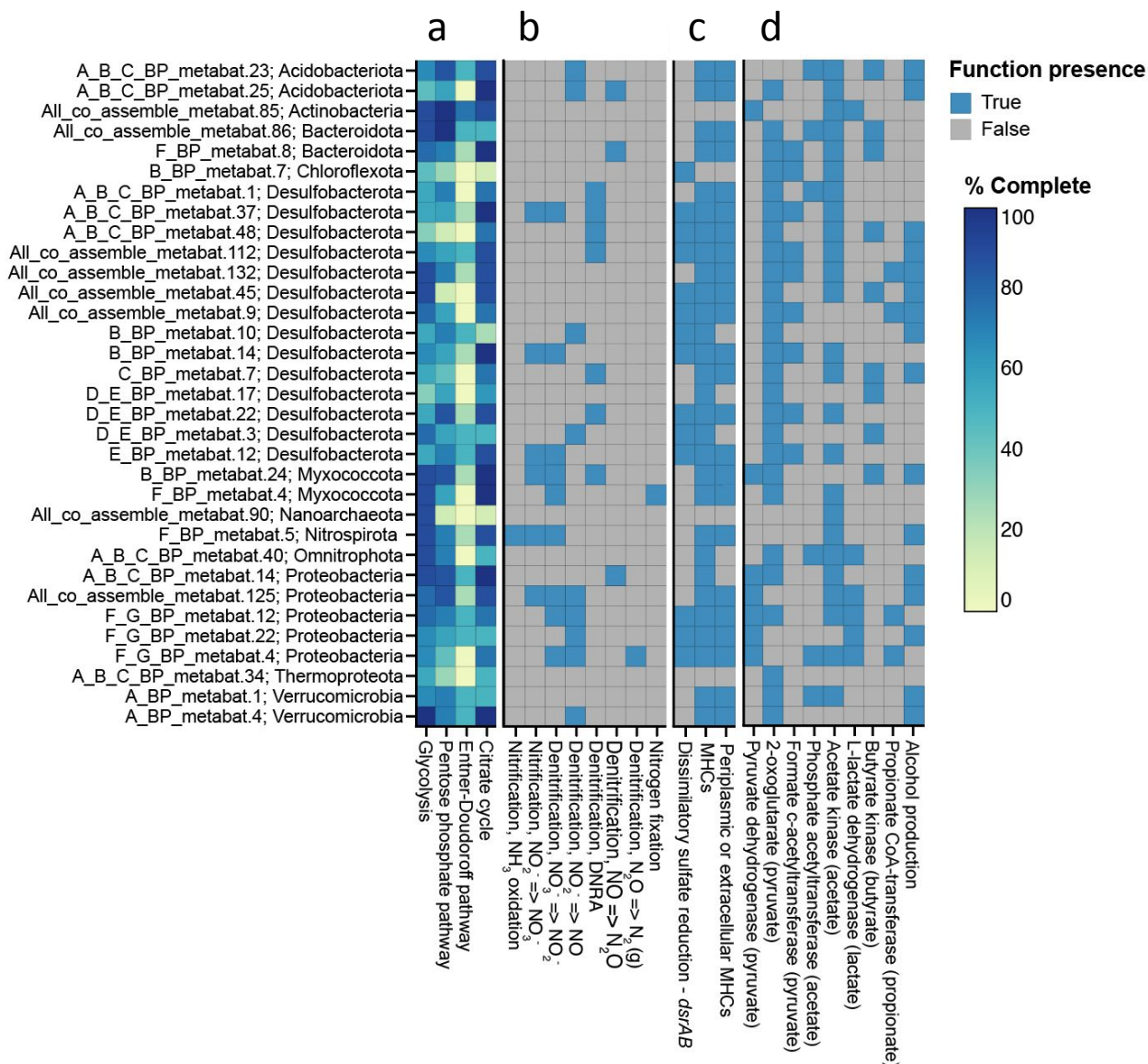


Fig. 6: Broad overview of the (a) completeness or (b, c, d) presence/absence of functions of interest in the 33 MAGs (listed on the left). Panels overview (a) central metabolism pathways, (b) inorganic N metabolisms, (c) alternate electron acceptors, and (d) SCFA and alcohol conversions. In D, the compound that the enzyme acts upon is in parentheses. Figure adapted from DRAM product.⁸⁸

Although there is clear evidence for accumulation of unique aromatic compounds within the beaver ponds (**Fig. 5**), none of the MAGs in this study encoded the enzymatic machinery for anaerobic degradation of aromatic C, which is often formed during soil heating. For example, the enzyme benzylsuccinate synthase (EC:4.1.99.11) that catalyzes fumarate addition as the first step of anaerobic toluene catabolism was absent from all the reconstructed MAGs.¹¹⁶ Only one MAG (B_BP_metabat.7; phyla *Chloroflexota*) encoded a benzylsuccinate CoA-transferase subunit (EC:2.8.3.15), which catalyzes the next step of the degradation reaction. Therefore, we infer that the anaerobic degradation of aromatic compounds is likely not a widespread metabolism in the

1
2
3 beaver pond microbiome. Because pyDOM is rich in aromatic structures,¹¹⁷ these results could
4 explain why these molecules appear to be enriched in the low-oxygen beaver ponds (**Fig. 4**).

5
6 Conversely, there is evidence for the potential utilization of other likely more labile
7 compounds generated indirectly following wildfire through microbial degradation of necromass-
8 derived C via the utilization of peptidases; all 33 of the MAGs encoded peptidases, with an average
9 of ~116 per genome. Peptidases in the families S33 and C26 were among the most encoded (298
10 and 219 encoded genes, respectively), similar to other freshwater studies (Wilkins, unpublished
11 data). Peptidases within the S33 family release the N-terminal residue from a peptide, and C26
12 peptides cleave gamma-linked glutamate bonds. Another top represented family is the M23B
13 family, which contains endopeptidases which lyse bacterial cell wall peptidoglycans. Previous
14 studies have discussed the potential lysing of heat-sensitive cells during fire, which may lead to
15 the release of microbially-derived C after wildfire.^{118,119} The encoding of peptidases within our
16 MAG database adds to the hypothesis that post-fire taxa may use this necromass-derived C, which
17 is more labile than aromatic C, following wildfire. From these observations, we infer that the
18 beaver pond microbiome is likely degrading necromass derived from heat-sensitive microbial or
19 invertebrate soil fauna from the surrounding burned watershed,¹²⁰ rather than relying on pyDOM
20 or limited vegetation inputs as the primary source of C. Although this has been shown in soils,³⁴ it
21 has yet to be shown in wetlands within burn scars. These observations also further explain the
22 enrichment of aromatic DOM in the beaver ponds, which is often associated with pyDOM.
23
24

25 The microbial taxa discussed here (e.g., Desulfobacterota) are not typically found in free-
26 flowing freshwater systems^{121,122} or fire-impacted soils,¹²³ demonstrating that microbiomes within
27 beaver pond sediments have the potential to perform unique biogeochemical reactions within the
28 watershed, thus enhancing the ability of these features to act as ecosystem control points. The
29 functional potential of the dominant community members in these burned beaver complex systems
30 may contribute to metal mobilization through the stream (**Fig. S8**) and highly reducing
31 metabolisms might also facilitate the local sequestration of DOC and DON seen through the
32 complex (**Fig. 4**). Thus, the implications of potential microbially-mediated heavy metal
33 transformations are a key area for future research in fire-impacted wetlands. While we recognize
34 the relatively small number of samples in our analysis, we believe that this study emphasizes the
35 importance of beaver ponds on the biogeochemical processing of burned areas and represents an
36 important step towards understanding how pyDOM is cycled in low-oxygen wetland
37 environments.
38
39
40

41 **4. Conclusions**

42 Water chemistry and microbiology indeed change as water flows through a fire-impacted
43 region, due to the combined influence of fire-impacted DOM and the presence of beaver ponds
44 along the stream channel. These burned beaver ponds had higher DOC, DTN, and nitrate compared
45 to an upstream reach or an adjacent unburned stream. There was a pattern of increased DOC and
46 DTN within the ponds compared to free-flowing streams and nitrate appeared to decline as water
47 moved through the sequence of beaver ponds. There were more N-containing formulas detected
48 in the ponds and lower C:N ratios, which would be consistent with increased DTN retention. In
49 addition to the increase in N-containing compounds, surface water in the beaver ponds had lower
50 C:N ratios and higher aromaticity than burned stream water. Impoundment within beaver ponds
51 may enhance post-fire sediment and C and N storage compared to free-flowing streams, which
52 may minimize the downstream formation of carcinogenic disinfection by-products during
53 chlorination at water treatment plants.^{101,124} Microbial analyses indicated that the input of fresh
54
55
56
57
58
59
60

pyDOM did not significantly impact the dominant phyla in the beaver ponds. Rather than using aromatic pyDOM as the primary source of C for respiration, microbes in these sites likely degrade biomass and other more labile sources of organic C. The preservation of pyDOM appeared to be localized within the ponds themselves as changes in elemental composition and unique formulas were limited to the ponds and not observed downstream; therefore, fire-impacted beaver ponds appear to function as biogeochemical “hotspots” due to their unique geochemistry and microbiomes.

Author Information

Corresponding Author: Thomas Borch

Phone: 970-491-6235

Email: Thomas.borch@colostate.edu

Acknowledgement

Stream water DOC, DTN was conducted at the Rocky Mountain Research Station, biogeochemistry laboratory, courtesy of the USDA Forest Service. The authors also acknowledge support to MJW and TB from the National Science Foundation under Grant Number 1512670 and USDA National Institute of Food Agriculture through AFRI grant no. 2021-67019034608. This research was funded by the National Science Foundation (2114868) and AFRI grant no. 2021-67019-33726 from the USDA National Institute of Food and Agriculture. A portion of this work was performed at the National High Magnetic Field Laboratory ICR User Facility, which is supported by the National Science Foundation Division of Chemistry and Division of Materials Research through DMR-1644779 and the State of Florida. This work was additionally supported through a grant to MJW, TB and CCR from the Colorado Water Center. TOC art was created with [BioRender.com](https://www.biorender.com).

References

- (1) McDonald, R.; Shemie, D. *Urban Water Blueprint: Mapping Conservation Solutions to the Global Water Challenge.*; Washington, D.C., 2014.
- (2) de Groot, R.; D’Arge, R.; Sutton, P.; Grasso, M.; Limburg, K.; Farber, S.; Raskin, R.; van den Belt, M.; Costanza, R.; Hannon, B.; Paruelo, J.; O’Neill, R.; Naeem, S. The Value of the the World’s Ecosystem Services and Natural Capital. *Nature* **2003**, No. 387, 253–260.
- (3) Stein, S. M.; Butler, B. Private Forests and Public Resources. *Wildland Waters* **2004**, Summer (FS 790), 1–24. <https://doi.org/10.1034/j.1399-3038.2001.012004179-.x>.
- (4) Bladon, K. D.; Emelko, M. B.; Silins, U.; Stone, M. Wildfire and the Future of Water Supply. *Environmental Science and Technology* **2014**, 48 (16), 8936–8943. <https://doi.org/10.1021/es500130g>.
- (5) Ramchander, M.; Rahul, K. Microbial Diversity of Wetlands of India. *Research Journal of Chemistry and Environment Vol* **2021**, 25 (3).
- (6) Emelko, M. B.; Silins, U.; Bladon, K. D.; Stone, M. Implications of Land Disturbance on Drinking Water Treatability in a Changing Climate: Demonstrating the Need for “ Source Water Supply and Protection” Strategies. *Water Research* **2011**, 45 (2), 461–472. <https://doi.org/10.1016/j.watres.2010.08.051>.
- (7) Alizadeh, M. R.; Abatzoglou, J. T.; Luce, C. H.; Adamowski, J. F.; Farid, A.; Sadegh, M. Warming Enabled Upslope Advance in Western US Forest Fires. **2021**, 118. <https://doi.org/10.1073/pnas.2009717118/-/DCSupplemental>.

- 1
2
3 (8) Abatzoglou, J. T.; Kolden, C. A.; Williams, A. P.; Lutz, J. A.; Smith, A. M. S. Climatic
4 Influences on Interannual Variability in Regional Burn Severity across Western US
5 Forests. *International Journal of Wildland Fire* **2017**, *26* (4), 269–275.
6 <https://doi.org/10.1071/WF16165>.
7
8 (9) Knicker, H. How Does Fire Affect the Nature and Stability of Soil Organic Nitrogen and
9 Carbon? A Review. *Biogeochemistry* **2007**, *85* (1), 91–118.
10 <https://doi.org/10.1007/s10533-007-9104-4>.
11
12 (10) Bird, M. I.; Wynn, J. G.; Saiz, G.; Wurster, C. M.; McBeath, A. The Pyrogenic Carbon Cycle.
13 *Annual Review of Earth and Planetary Sciences* **2015**, *43*, 273–298.
14 <https://doi.org/10.1146/annurev-earth-060614-105038>.
15
16 (11) Viedma, O.; Quesada, J.; Torres, I.; de Santis, A.; Moreno, J. M. Fire Severity in a Large
17 Fire in a Pinus Pinaster Forest Is Highly Predictable from Burning Conditions, Stand
18 Structure, and Topography. *Ecosystems* **2015**, *18* (2), 237–250.
19 <https://doi.org/10.1007/s10021-014-9824-y>.
20
21 (12) Doerr, S. H.; Santín, C. Global Trends in Wildfire and Its Impacts: Perceptions versus
22 Realities in a Changing World. *Philosophical Transactions of the Royal Society B:*
23 *Biological Sciences* **2016**, *371* (1696). <https://doi.org/10.1098/rstb.2015.0345>.
24
25 (13) Schmidt, M. W. I.; Noack, A. G. Black Carbon in Soils and Sediments: Analysis,
26 Distribution, Implications, and Current Challenges. *Global Biogeochemical Cycles*.
27 Blackwell Publishing Ltd September 1, 2000, pp 777–793.
28 <https://doi.org/10.1029/1999GB001208>.
29
30 (14) Olivella, M. A.; Ribalta, T. G.; De Febrer, A. R.; Mollet, J. M.; De Las Heras, F. X. C.
31 Distribution of Polycyclic Aromatic Hydrocarbons in Riverine Waters after Mediterranean
32 Forest Fires. *Science of the Total Environment* **2006**, *355* (1–3), 156–166.
33 <https://doi.org/10.1016/j.scitotenv.2005.02.033>.
34
35 (15) Rhoades, C. C.; Chow, A. T.; Covino, T. P.; Feghel, T. S.; Pierson, D. N.; Rhea, A. E. The
36 Legacy of a Severe Wildfire on Stream Nitrogen and Carbon in Headwater Catchments.
37 *Ecosystems* **2018**. <https://doi.org/10.1007/s10021-018-0293-6>.
38
39 (16) Rhoades, C. C.; Nunes, J. P.; Silins, U.; Doerr, S. H. The Influence of Wildfire on Water
40 Quality and Watershed Processes: New Insights and Remaining Challenges. *International*
41 *Journal of Wildland Fire* **2019**, *28* (10), 721–725. https://doi.org/10.1071/WFv28n10_FO.
42
43 (17) Minshall, G. W.; Brock, J. T.; Andrews, D. A.; Robinson, C. T. Water Quality, Substratum
44 and Biotic Responses of Five Central Idaho (USA) Streams during the First Year Following
45 the Mortar Creek Fire. *International Journal of Wildland Fire* **2001**, *10* (2), 185–199.
46 <https://doi.org/10.1071/WF01017>.
47
48 (18) Murphy, S. F.; Writer, J. H.; McCleskey, R. B.; Martin, D. A. The Role of Precipitation Type,
49 Intensity, and Spatial Distribution in Source Water Quality after Wildfire. *Environmental*
50 *Research Letters* **2015**, *10* (8). <https://doi.org/10.1088/1748-9326/11/7/079501>.
51
52 (19) Hohner, A. K.; Cawley, K.; Oropeza, J.; Summers, R. S.; Rosario-Ortiz, F. L. Drinking Water
53 Treatment Response Following a Colorado Wildfire. *Water Research* **2016**, *105*, 187–198.
54 <https://doi.org/10.1016/j.watres.2016.08.034>.
55
56 (20) Ferrer, I.; Thurman, E. M.; Zweigenbaum, J. A.; Murphy, S. F.; Webster, J. P.; Rosario-
57 Ortiz, F. L. Wildfires: Identification of a New Suite of Aromatic Polycarboxylic Acids in Ash
58
59
60

- 1
2
3 and Surface Water. *Science of the Total Environment* **2021**, 770.
4 <https://doi.org/10.1016/j.scitotenv.2020.144661>.
- 5
6 (21) Smith, H. G.; Sheridan, G. J.; Lane, P. N. J.; Nyman, P.; Haydon, S. Wildfire Effects on
7 Water Quality in Forest Catchments: A Review with Implications for Water Supply.
8 *Journal of Hydrology*. January 5, 2011, pp 170–192.
9 <https://doi.org/10.1016/j.jhydrol.2010.10.043>.
- 10
11 (22) Kleber, M. What Is Recalcitrant Soil Organic Matter? *Environmental Chemistry* **2010**, 7
12 (4), 320–332. <https://doi.org/10.1071/EN10006>.
- 13
14 (23) Lehmann, J.; Kleber, M. The Contentious Nature of Soil Organic Matter. *Nature* **2015**, 528
15 (7580), 60–68. <https://doi.org/10.1038/nature16069>.
- 16
17 (24) Robinne, F. N.; Bladon, K. D.; Miller, C.; Parisien, M. A.; Mathieu, J.; Flannigan, M. D. A
18 Spatial Evaluation of Global Wildfire-Water Risks to Human and Natural Systems. *Science*
19 *of the Total Environment* **2018**, 610–611, 1193–1206.
20 <https://doi.org/10.1016/j.scitotenv.2017.08.112>.
- 21
22 (25) Naiman, R. J.; Johnston, C. A.; Kelley, J. C. Alteration of North American Streams by
23 Beaver. *BioScience* **1988**, 38 (11), 753–762. <https://doi.org/10.2307/1310784>.
- 24
25 (26) Rosell, F.; Bozsér, O.; Collen, P.; Parker, H. Ecological Impact of Beavers Castor Fiber and
26 Castor Canadensis and Their Ability to Modify Ecosystems. *Mammal Review* **2005**, 35 (3–
27 4), 248–276. <https://doi.org/10.1111/j.1365-2907.2005.00067.x>.
- 28
29 (27) Briggs, M. A.; Wang, C.; Day-Lewis, F. D.; Williams, K. H.; Dong, W.; Lane, J. W. Return
30 Flows from Beaver Ponds Enhance Floodplain-to-River Metals Exchange in Alluvial
31 Mountain Catchments. *Science of the Total Environment* **2019**, 685, 357–369.
32 <https://doi.org/10.1016/j.scitotenv.2019.05.371>.
- 33
34 (28) Boye, K.; Herrmann, A. M.; Schaefer, M. v.; Tfaily, M. M.; Fendorf, S. Discerning
35 Microbially Mediated Processes during Redox Transitions in Flooded Soils Using Carbon
36 and Energy Balances. *Frontiers in Environmental Science* **2018**, 6 (MAY).
37 <https://doi.org/10.3389/fenvs.2018.00015>.
- 38
39 (29) Larsen, A.; Larsen, J. R.; Lane, S. N. Dam Builders and Their Works: Beaver Influences on
40 the Structure and Function of River Corridor Hydrology, Geomorphology,
41 Biogeochemistry and Ecosystems. *Earth-Science Reviews*. Elsevier B.V. July 1, 2021.
42 <https://doi.org/10.1016/j.earscirev.2021.103623>.
- 43
44 (30) Missik, J. E. C.; Liu, H.; Gao, Z.; Huang, M.; Chen, X.; Arntzen, E.; Mcfarland, D. P.; Ren, H.;
45 Titzler, P. S.; Thomle, J. N.; Goldman, A. Groundwater-River Water Exchange Enhances
46 Growing Season Evapotranspiration and Carbon Uptake in a Semiarid Riparian
47 Ecosystem. *Journal of Geophysical Research: Biogeosciences* **2019**, 124 (1), 99–114.
48 <https://doi.org/10.1029/2018JG004666>.
- 49
50 (31) Lynch, L. M.; Covino, T. P.; Boot, C. M.; Wallenstein, M. D.; Sutfin, N. A.; Feghel, T. S. River
51 Channel Connectivity Shifts Metabolite Composition and Dissolved Organic Matter
52 Chemistry. *Nature Communications* **2019**, 10 (1). <https://doi.org/10.1038/s41467-019-08406-8>.
- 53
54 (32) Wegener, P.; Covino, T.; Rhoades, C. Evaluating Controls on Nutrient Retention and
55 Export in Wide and Narrow Valley Segments of a Mountain River Corridor. *Journal of*
56 *Geophysical Research: Biogeosciences* **2018**, 123 (6), 1817–1826.
57 <https://doi.org/10.1029/2017JG004109>.
- 58
59
60

- 1
2
3 (33) Fischer, M. S.; Stark, F. G.; Berry, T. D.; Zeba, N.; Whitman, T.; Traxler, M. F. Pyrolyzed
4 Substrates Induce Aromatic Compound Metabolism in the Post-Fire Fungus, *Pyronema*
5 *Domesticum*. *Frontiers in Microbiology* **2021**, *12*.
6 <https://doi.org/10.3389/fmicb.2021.729289>.
7
8 (34) Nelson, A. R.; Narrowe, A. B.; Rhoades, C. C.; Fegel, T. S.; Roth, H. K.; Chu, R. K.;
9 Amundson, K. K.; Geonczy, S. E.; Young, R. B.; Steindorff, A. S.; Mondo, S. J.; Grigoriev, I.
10 v; Salamov, A.; Borch, T.; Wilkins, M. J.; author, C. Playing with FiRE: A Genome Resolved
11 View of the Soil Microbiome Responses to High Severity Forest Wildfire. *bioRxiv* **2021**.
12 <https://doi.org/10.1101/2021.08.17.456416>.
13
14 (35) Whitfield, C. J.; Baulch, H. M.; Chun, K. P.; Westbrook, C. J. Beaver-Mediated Methane
15 Emission: The Effects of Population Growth in Eurasia and the Americas. *Ambio* **2015**, *44*
16 (1), 7–15. <https://doi.org/10.1007/s13280-014-0575-y>.
17
18 (36) Halley, D. J.; Saveljev, A. P.; Rosell, F. Population and Distribution of Beavers *Castor Fiber*
19 and *Castor Canadensis* in Eurasia. *Mammal Review*. Blackwell Publishing Ltd January 1,
20 2021, pp 1–24. <https://doi.org/10.1111/mam.12216>.
21
22 (37) Geisseler, D.; Horwath, W. R.; Joergensen, R. G.; Ludwig, B. Pathways of Nitrogen
23 Utilization by Soil Microorganisms - A Review. *Soil Biology and Biochemistry*. December
24 2010, pp 2058–2067. <https://doi.org/10.1016/j.soilbio.2010.08.021>.
25
26 (38) Acquisti, C.; Elser, J. J.; Kumar, S. Ecological Nitrogen Limitation Shapes the DNA
27 Composition of Plant Genomes. *Molecular Biology and Evolution* **2009**, *26* (5), 953–956.
28 <https://doi.org/10.1093/molbev/msp038>.
29
30 (39) Adkins, J.; Sanderman, J.; Miesel, J. Soil Carbon Pools and Fluxes Vary across a Burn
31 Severity Gradient Three Years after Wildfire in Sierra Nevada Mixed-Conifer Forest.
32 *Geoderma* **2019**, *333*, 10–22. <https://doi.org/10.1016/j.geoderma.2018.07.009>.
33
34 (40) Miesel, J. R.; Hockaday, W. C.; Kolka, R. K.; Townsend, P. A. Soil Organic Matter
35 Composition and Quality across Fire Severity Gradients in Coniferous and Deciduous
36 Forests of the Southern Boreal Region. *Journal of Geophysical Research G:*
37 *Biogeosciences* **2015**, *120* (6), 1124–1141. <https://doi.org/10.1002/2015JG002959>.
38
39 (41) Rhoades, C. C.; Entwistle, D.; Butler, D. The Influence of Wildfire Extent and Severity on
40 Streamwater Chemistry, Sediment and Temperature Following the Hayman Fire,
41 Colorado. *International Journal of Wildland Fire* **2011**, *20* (3), 430–442.
42 <https://doi.org/10.1071/WF09086>.
43
44 (42) Bladon, K. D.; Silins, U.; Wagner, M. J.; Stone, M.; Emelko, M. B.; Mendoza, C. A.; Devito,
45 K. J.; Boon, S. Wildfire Impacts on Nitrogen Concentration and Production from
46 Headwater Streams in Southern Alberta's Rocky Mountains. *Canadian Journal of Forest*
47 *Research* **2008**, *38* (9), 2359–2371. <https://doi.org/10.1139/X08-071>.
48
49 (43) Robinne, F. N.; Bladon, K. D.; Silins, U.; Emelko, M. B.; Flannigan, M. D.; Parisien, M. A.;
50 Wang, X.; Kienzle, S. W.; Dupont, D. P. A Regional-Scale Index for Assessing the Exposure
51 of Drinking-Water Sources to Wildfires. *Forests* **2019**, *10* (5), 1–21.
52 <https://doi.org/10.3390/f10050384>.
53
54 (44) Pisani, O.; Boyer, J. N.; Podgorski, D. C.; Thomas, C. R.; Coley, T.; Jaffé, R. Molecular
55 Composition and Bioavailability of Dissolved Organic Nitrogen in a Lake Flow-Influenced
56 River in South Florida, USA. *Aquatic Sciences* **2017**, *79* (4), 891–908.
57 <https://doi.org/10.1007/s00027-017-0540-5>.
58
59
60

- 1
2
3 (45) Hertkorn, N.; Harir, M.; Cawley, K. M.; Schmitt-Kopplin, P.; Jaffé, R. Molecular
4 Characterization of Dissolved Organic Matter from Subtropical Wetlands: A Comparative
5 Study through the Analysis of Optical Properties, NMR and FTICR/MS. *Biogeosciences*
6 **2016**, *13* (8), 2257–2277. <https://doi.org/10.5194/bg-13-2257-2016>.
7
8 (46) Roth, H. K.; Borch, T.; Young, R. B.; Bahureksa, W.; Blakney, G. T.; Nelson, A. R.; Wilkins,
9 M. J.; McKenna, A. M. Enhanced Speciation of Pyrogenic Organic Matter from Wildfires
10 Enabled by 21 T FT-ICR Mass Spectrometry. *Analytical Chemistry* **2022**,
11 [acs.analchem.1c05018](https://doi.org/10.1021/acs.analchem.1c05018). <https://doi.org/10.1021/acs.analchem.1c05018>.
12
13 (47) Jiménez-Morillo, N. T.; de la Rosa, J. M.; Waggoner, D.; Almendros, G.; González-Vila, F.
14 J.; González-Pérez, J. A. Fire Effects in the Molecular Structure of Soil Organic Matter
15 Fractions under Quercus Suber Cover. *Catena (Amst)* **2016**, *145*, 266–273.
16 <https://doi.org/10.1016/j.catena.2016.06.022>.
17
18 (48) Luo, L.; Chen, Z.; Lv, J.; Cheng, Y.; Wu, T.; Huang, R. Molecular Understanding of Dissolved
19 Black Carbon Sorption in Soil-Water Environment. *Water Research* **2019**, *154*, 210–216.
20 <https://doi.org/10.1016/j.watres.2019.01.060>.
21
22 (49) de la Rosa, J. M.; Knicker, H. Bioavailability of N Released from N-Rich Pyrogenic Organic
23 Matter: An Incubation Study. *Soil Biology and Biochemistry* **2011**, *43* (12), 2368–2373.
24 <https://doi.org/10.1016/j.soilbio.2011.08.008>.
25
26 (50) Mcknight, D. M.; Boyer, E. W.; Westerhoff, P. K.; Doran, P. T.; Kulbe, T.; Andersen, D. T.
27 *Spectrofluorometric Characterization of Dissolved Organic Matter for Indication of*
28 *Precursor Organic Material and Aromaticity*; 2001; Vol. 46.
29
30 (51) Jaffé, R.; McKnight, D.; Maie, N.; Cory, R.; McDowell, W. H.; Campbell, J. L. Spatial and
31 Temporal Variations in DOM Composition in Ecosystems: The Importance of Long-Term
32 Monitoring of Optical Properties. *Journal of Geophysical Research: Biogeosciences* **2008**,
33 *113* (4), 1–15. <https://doi.org/10.1029/2008JG000683>.
34
35 (52) Rosario-Ortiz, F. L.; Korak, J. A. Oversimplification of Dissolved Organic Matter
36 Fluorescence Analysis: Potential Pitfalls of Current Methods. *Environmental Science and*
37 *Technology* **2017**, *51* (2), 759–761. <https://doi.org/10.1021/acs.est.6b06133>.
38
39 (53) Cawley, K. M.; Hohner, A. K.; McKee, G. A.; Borch, T.; Omur-Ozbek, P.; Oropeza, J.;
40 Rosario-Ortiz, F. L. Characterization and Spatial Distribution of Particulate and Soluble
41 Carbon and Nitrogen from Wildfire-Impacted Sediments. *Journal of Soils and Sediments*
42 **2018**, *18* (4), 1314–1326. <https://doi.org/10.1007/s11368-016-1604-1>.
43
44 (54) Cory, R. M.; McKnight, D. M. Fluorescence Spectroscopy Reveals Ubiquitous Presence of
45 Oxidized and Reduced Quinones in Dissolved Organic Matter. *Environmental Science &*
46 *Technology* **2005**, *39* (21), 8142–8149. <https://doi.org/10.1021/es0506962>.
47
48 (55) Parlanti, E.; Woè Rz, K.; GeoÉroy, L.; Lamotte, M. Dissolved Organic Matter Fluorescence
49 Spectroscopy as a Tool to Estimate Biological Activity in a Coastal Zone Submitted to
50 Anthropogenic Inputs. *Organic Geochemistry* **2000**, 1765–1781.
51 [https://doi.org/10.1016/S0146-6380\(00\)00124-8](https://doi.org/10.1016/S0146-6380(00)00124-8).
52
53 (56) Bahureksa, W.; Tfaily, M. M.; Boiteau, R. M.; Young, R. B.; Logan, M. N.; McKenna, A. M.;
54 Borch, T. Soil Organic Matter Characterization by Fourier Transform Ion Cyclotron
55 Resonance Mass Spectrometry (FTICR MS): A Critical Review of Sample Preparation,
56 Analysis, and Data Interpretation. *Environmental Science and Technology*. American
57 Chemical Society July 20, 2021, pp 9637–9656. <https://doi.org/10.1021/acs.est.1c01135>.
58
59
60

- 1
2
3 (57) Hertkorn, N.; Frommberger, M.; Witt, M.; Koch, B. P.; Schmitt-Kopplin, P.; Perdue, E. M.
4 Natural Organic Matter and the Event Horizon of Mass Spectrometry. *Analytical*
5 *Chemistry* **2008**, *80* (23), 8908–8919. <https://doi.org/10.1021/ac800464g>.
6
7 (58) Hendrickson, C. L.; Quinn, J. P.; Kaiser, N. K.; Smith, D. F.; Blakney, G. T.; Chen, T.;
8 Marshall, A. G.; Weisbrod, C. R.; Beu, S. C. 21 Tesla Fourier Transform Ion Cyclotron
9 Resonance Mass Spectrometer: A National Resource for Ultrahigh Resolution Mass
10 Analysis. *J Am Soc Mass Spectrom* **2015**, *26* (9), 1626–1632.
11 <https://doi.org/10.1007/s13361-015-1182-2>.
12
13 (59) Ohno, T.; Slichter, R. L.; Hatcher, P. G. Comparative Study of Organic Matter Chemical
14 Characterization Using Negative and Positive Mode Electrospray Ionization Ultrahigh-
15 Resolution Mass Spectrometry. *Analytical and Bioanalytical Chemistry* **2016**, *408* (10),
16 2497–2504. <https://doi.org/10.1007/s00216-016-9346-x>.
17
18 (60) Dittmar, T.; Koch, B.; Hertkorn, N.; Kattner, G. A Simple and Efficient Method for the
19 Solid-Phase Extraction of Dissolved Organic Matter (SPE-DOM) from Seawater. *Limnology*
20 *and Oceanography: Methods* **2008**, *6* (6), 230–235.
21 <https://doi.org/10.4319/lom.2008.6.230>.
22
23 (61) Dittmar, T.; Koch, B.; Hertkorn, N.; Kattner, G. A Simple and Efficient Method for the
24 Solid-Phase Extraction of Dissolved Organic Matter (SPE-DOM) from Seawater. *Limnology*
25 *and Oceanography: Methods* **2008**, *6*, 230–235.
26
27 (62) Lam, B.; Baer, A.; Alae, M.; Lefebvre, B.; Moser, A.; Williams, A.; Simpson, A. J. Major
28 Structural Components in Freshwater Dissolved Organic Matter. *Environmental Science*
29 *and Technology* **2007**, *41* (24), 8240–8247. <https://doi.org/10.1021/es0713072>.
30
31 (63) Li, Y.; Harir, M.; Uhl, J.; Kanawati, B.; Lucio, M.; Smirnov, K. S.; Koch, B. P.; Schmitt-
32 Kopplin, P.; Hertkorn, N. How Representative Are Dissolved Organic Matter (DOM)
33 Extracts? A Comprehensive Study of Sorbent Selectivity for DOM Isolation. *Water*
34 *Research* **2017**, *116*, 316–323. <https://doi.org/10.1016/j.watres.2017.03.038>.
35
36 (64) Emmett, M. R.; White, F. M.; Hendrickson, C. L.; Shi, D. H.; Marshall, A. G. Application of
37 Micro-Electrospray Liquid Chromatography Techniques to FT-ICR MS to Enable High-
38 Sensitivity Biological Analysis. *J Am Soc Mass Spectrom* **1998**, *9* (4), 333–340.
39 [https://doi.org/10.1016/S1044-0305\(97\)00287-0](https://doi.org/10.1016/S1044-0305(97)00287-0).
40
41 (65) Smith, D. F.; Podgorski, D. C.; Rodgers, R. P.; Blakney, G. T.; Hendrickson, C. L. 21 Tesla FT-
42 ICR Mass Spectrometer for Ultrahigh-Resolution Analysis of Complex Organic Mixtures.
43 *Analytical Chemistry* **2018**, *90* (3), 2041–2047.
44 <https://doi.org/10.1021/acs.analchem.7b04159>.
45
46 (66) Kaiser, N. K.; McKenna, A. M.; Savory, J. J.; Hendrickson, C. L.; Marshall, A. G. Tailored Ion
47 Radius Distribution for Increased Dynamic Range in FT-ICR Mass Analysis of Complex
48 Mixtures. *Analytical Chemistry* **2013**, *85* (1), 265–272.
49 <https://doi.org/10.1021/ac302678v>.
50
51 (67) Chen, T.; Beu, S. C.; Kaiser, N. K.; Hendrickson, C. L. Note: Optimized Circuit for Excitation
52 and Detection with One Pair of Electrodes for Improved Fourier Transform Ion Cyclotron
53 Resonance Mass Spectrometry. *Review of Scientific Instruments* **2014**, *85* (6).
54 <https://doi.org/10.1063/1.4883179>.
55
56 (68) Boldin, I. A.; Nikolaev, E. N. Fourier Transform Ion Cyclotron Resonance Cell with
57 Dynamic Harmonization of the Electric Field in the Whole Volume by Shaping of the
58
59
60

- 1
2
3
4
5
6
7
8
9
10
11
12
13
14
15
16
17
18
19
20
21
22
23
24
25
26
27
28
29
30
31
32
33
34
35
36
37
38
39
40
41
42
43
44
45
46
47
48
49
50
51
52
53
54
55
56
57
58
59
60
- Excitation and Detection Electrode Assembly. *Rapid Communications in Mass Spectrometry* **2011**, *25* (1), 122–126. <https://doi.org/10.1002/rcm.4838>.
- (69) Blakney, G. T.; Hendrickson, C. L.; Marshall, A. G. Predator Data Station: A Fast Data Acquisition System for Advanced FT-ICR MS Experiments. *International Journal of Mass Spectrometry* **2011**, *306* (2–3), 246–252. <https://doi.org/10.1016/j.ijms.2011.03.009>.
- (70) Xian, F.; Hendrickson, C. L.; Blakney, G. T.; Beu, S. C.; Marshall, A. G. Automated Broadband Phase Correction of Fourier Transform Ion Cyclotron Resonance Mass Spectra. *Analytical Chemistry* **2010**, *82* (21), 8807–8812. <https://doi.org/10.1021/ac101091w>.
- (71) Savory, J. J.; Kaiser, N. K.; Mckenna, A. M.; Xian, F.; Blakney, G. T.; Rodgers, R. P.; Hendrickson, C. L.; Marshall, A. G. Measurement Accuracy with a “Walking” Calibration Equation. *Analytical Chemistry* **2011**, *83*, 1732–1736.
- (72) Kendrick, E. A Mass Scale Based Resolution Mass Spectrometry of Organic Compounds. *Analytical Chemistry* **1963**, *35* (13), 2146–2154.
- (73) Hughey, C. A.; Hendrickson, C. L.; Rodgers, R. P.; Marshall, A. G.; Qian, K. Kendrick Mass Defect Spectrum: A Compact Visual Analysis for Ultrahigh-Resolution Broadband Mass Spectra. *Analytical Chemistry* **2001**, *73* (19), 4676–4681. <https://doi.org/10.1021/ac010560w>.
- (74) McLafferty, F. W.; Turecek, F. *Interpretation of Mass Spectra*, 4th ed.; University Science Books: Mill Valley, CA, 1993.
- (75) Corilo, Y. E. PetroOrg Software. Florida State University, Omics LLC: Tallahassee, FL 2014.
- (76) Koch, B. P.; Dittmar, T. From Mass to Structure: An Aromaticity Index for High-Resolution Mass Data of Natural Organic Matter. *Rapid Communications in Mass Spectrometry* **2006**, *20* (5), 926–932. <https://doi.org/10.1002/rcm.2386>.
- (77) Koch, B. P.; Dittmar, T. Erratum: From Mass to Structure: An Aromaticity Index for High-Resolution Mass Data of Natural Organic Matter (Rapid Communications in Mass Spectrometry (2006) 20 (926-932) DOI: 10.1002/Rcm.2386). *Rapid Communications in Mass Spectrometry* **2016**, *30* (1), 250. <https://doi.org/10.1002/rcm.7433>.
- (78) LaRowe, D. E.; Van Cappellen, P. Degradation of Natural Organic Matter: A Thermodynamic Analysis. *Geochimica et Cosmochimica Acta* **2011**, *75* (8), 2030–2042. <https://doi.org/10.1016/j.gca.2011.01.020>.
- (79) Kim, S.; Kramer, R. W.; Hatcher, P. G. Graphical Method for Analysis of Ultrahigh-Resolution Broadband Mass Spectra of Natural Organic Matter, the Van Krevelen Diagram. *Analytical Chemistry* **2003**, *75* (20), 5336–5344. <https://doi.org/10.1021/ac034415p>.
- (80) Quast, C.; Pruesse, E.; Yilmaz, P.; Gerken, J.; Schweer, T.; Yarza, P.; Peplies, J.; Glöckner, F. O. The SILVA Ribosomal RNA Gene Database Project: Improved Data Processing and Web-Based Tools. *Nucleic Acids Research* **2012**, *41* (D1), D590–D596. <https://doi.org/10.1093/nar/gks1219>.
- (81) Quast, C.; Pruesse, E.; Yilmaz, P.; Gerken, J.; Schweer, T.; Yarza, P.; Peplies, J.; Glöckner, F. O. The SILVA Ribosomal RNA Gene Database Project: Improved Data Processing and Web-Based Tools. *Nucleic Acids Research* **2013**, *41* (D1). <https://doi.org/10.1093/nar/gks1219>.

- 1
2
3 (82) Joshi, N.; Fass, J. Sickle: A Sliding-Window, Adaptive, Quality-Based Trimming Tool for
4 FastQ Files. 2011.
- 5 (83) Li, D.; Liu, C. M.; Luo, R.; Sadakane, K.; Lam, T. W. MEGAHIT: An Ultra-Fast Single-Node
6 Solution for Large and Complex Metagenomics Assembly via Succinct de Bruijn Graph.
7 *Bioinformatics* **2015**, *31* (10), 1674–1676.
8 <https://doi.org/10.1093/bioinformatics/btv033>.
- 9 (84) Kang, D. D.; Li, F.; Kirton, E.; Thomas, A.; Egan, R.; An, H.; Wang, Z. MetaBAT 2: An
10 Adaptive Binning Algorithm for Robust and Efficient Genome Reconstruction from
11 Metagenome Assemblies. *PeerJ* **2019**, *2019* (7). <https://doi.org/10.7717/peerj.7359>.
- 12 (85) Parks, D. H.; Imelfort, M.; Skennerton, C. T.; Hugenholtz, P.; Tyson, G. W. CheckM:
13 Assessing the Quality of Microbial Genomes Recovered from Isolates, Single Cells, and
14 Metagenomes. *Genome Research* **2015**, *25* (7), 1043–1055.
15 <https://doi.org/10.1101/gr.186072.114>.
- 16 (86) Chaumeil, P. A.; Mussig, A. J.; Hugenholtz, P.; Parks, D. H. GTDB-Tk: A Toolkit to Classify
17 Genomes with the Genome Taxonomy Database. *Bioinformatics* **2020**, *36* (6), 1925–
18 1927. <https://doi.org/10.1093/bioinformatics/btz848>.
- 19 (87) Olm, M. R.; Brown, C. T.; Brooks, B.; Banfield, J. F. DRep: A Tool for Fast and Accurate
20 Genomic Comparisons That Enables Improved Genome Recovery from Metagenomes
21 through de-Replication. *ISME Journal* **2017**, *11* (12), 2864–2868.
22 <https://doi.org/10.1038/ismej.2017.126>.
- 23 (88) Shaffer, M.; Borton, M. A.; McGivern, B. B.; Zayed, A. A.; la Rosa, S. L. 0003 3527 8101;
24 Solden, L. M.; Liu, P.; Narrowe, A. B.; Rodríguez-Ramos, J.; Bolduc, B.; Gazitúa, M. C.;
25 Daly, R. A.; Smith, G. J.; Vik, D. R.; Pope, P. B.; Sullivan, M. B.; Roux, S.; Wrighton, K. C.
26 DRAM for Distilling Microbial Metabolism to Automate the Curation of Microbiome
27 Function. *Nucleic Acids Research* **2020**, *48* (16), 8883–8900.
28 <https://doi.org/10.1093/nar/gkaa621>.
- 29 (89) Yu, N. Y.; Wagner, J. R.; Laird, M. R.; Melli, G.; Rey, S.; Lo, R.; Dao, P.; Cenk Sahinalp, S.;
30 Ester, M.; Foster, L. J.; Brinkman, F. S. L. PSORTb 3.0: Improved Protein Subcellular
31 Localization Prediction with Refined Localization Subcategories and Predictive
32 Capabilities for All Prokaryotes. *Bioinformatics* **2010**, *26* (13), 1608–1615.
33 <https://doi.org/10.1093/bioinformatics/btq249>.
- 34 (90) Harris, D. C. *Exploring Chemical Analysis*, Fifth Edition.; Fiorillo, J., Murphy, B., Hadler, G.
35 L., Simpson, J., Szczepanski, T., Eds.; W.H. Freeman and Company: New York, 2013.
- 36 (91) Wagner, S.; Jaffé, R.; Cawley, K.; Dittmar, T.; Stubbins, A. Associations between the
37 Molecular and Optical Properties of Dissolved Organic Matter in the Florida Everglades, a
38 Model Coastal Wetland System. *Frontiers in Chemistry* **2015**, *3* (NOV), 1–14.
39 <https://doi.org/10.3389/fchem.2015.00066>.
- 40 (92) Catalán, N.; Herrero Ortega, S.; Gröntoft, H.; Hilmarsson, T. G.; Bertilsson, S.; Wu, P.;
41 Levanoni, O.; Bishop, K.; Bravo, A. G. Effects of Beaver Impoundments on Dissolved
42 Organic Matter Quality and Biodegradability in Boreal Riverine Systems. *Hydrobiologia*
43 **2017**, *793* (1), 135–148. <https://doi.org/10.1007/s10750-016-2766-y>.
- 44 (93) Nummi, P.; Vehkaoja, M.; Pumpanen, J.; Ojala, A. Beavers Affect Carbon
45 Biogeochemistry: Both Short-Term and Long-Term Processes Are Involved. *Mammal*
46 *Review* **2018**, *48* (4), 298–311. <https://doi.org/10.1111/mam.12134>.
- 47
48
49
50
51
52
53
54
55
56
57
58
59
60

- 1
2
3 (94) Brust, G. E. Management Strategies for Organic Vegetable Fertility. In *Safety and Practice*
4 *for Organic Food*; Elsevier, 2019; pp 193–212. [https://doi.org/10.1016/B978-0-12-](https://doi.org/10.1016/B978-0-12-812060-6.00009-X)
5 [812060-6.00009-X](https://doi.org/10.1016/B978-0-12-812060-6.00009-X).
6
7 (95) Certini, G. Effects of Fire on Properties of Forest Soils: A Review. *Oecologia* **2005**, *143* (1),
8 1–10. <https://doi.org/10.1007/s00442-004-1788-8>.
9
10 (96) Wan, S.; Hui, D.; Luo, Y. *FIRE EFFECTS ON NITROGEN POOLS AND DYNAMICS IN*
11 *TERRESTRIAL ECOSYSTEMS: A META-ANALYSIS*; 2001; Vol. 11.
12 (97) Noël, V.; Tfaily, M. M.; Fendorf, S.; Bone, S. E.; Boye, K.; Williams, K. H.; Bargar, J. R.
13 Thermodynamically Controlled Preservation of Organic Carbon in Floodplains. *Nature*
14 *Geoscience* **2017**, *10* (6), 415–419. <https://doi.org/10.1038/ngeo2940>.
15
16 (98) de La Rosa, J. M.; Miller, A. Z.; Knicker, H. Soil-Borne Fungi Challenge the Concept of
17 Long-Term Biochemical Recalcitrance of Pyrochar. *Scientific Reports* **2018**, *8* (1), 1–9.
18 <https://doi.org/10.1038/s41598-018-21257-5>.
19
20 (99) Faria, S. R.; de la Rosa, J. M.; Knicker, H.; González-Pérez, J. A.; Keizer, J. J. Molecular
21 Characterization of Wildfire Impacts on Organic Matter in Eroded Sediments and Topsoil
22 in Mediterranean Eucalypt Stands. *Catena (Amst)* **2015**, *135*, 29–37.
23 <https://doi.org/10.1016/j.catena.2015.07.007>.
24
25 (100) Knicker, H.; González-Vila, F. J.; Polvillo, O.; González, J. A.; Almendros, G. Fire-Induced
26 Transformation of C- and N- Forms in Different Organic Soil Fractions from a Dystric
27 Cambisol under a Mediterranean Pine Forest (*Pinus Pinaster*). *Soil Biology and*
28 *Biochemistry* **2005**, *37* (4), 701–718. <https://doi.org/10.1016/j.soilbio.2004.09.008>.
29
30 (101) Bahureksa, W.; Young, R. B.; McKenna, A. M.; Chen, H.; Thorn, K. A.; Rosario-Ortiz, F. L.;
31 Borch, T. Nitrogen Enrichment during Soil Organic Matter Burning and Molecular
32 Evidence of Maillard Reactions. *Environmental Science & Technology* **2022**,
33 [acs.est.1c06745](https://doi.org/10.1021/acs.est.1c06745). <https://doi.org/10.1021/acs.est.1c06745>.
34
35 (102) Rivas-Ubach, A.; Liu, Y.; Bianchi, T. S.; Tolić, N.; Jansson, C.; Paša-Tolić, L. Moving beyond
36 the van Krevelen Diagram: A New Stoichiometric Approach for Compound Classification
37 in Organisms. *Analytical Chemistry* **2018**, *90* (10), 6152–6160.
38 <https://doi.org/10.1021/acs.analchem.8b00529>.
39
40 (103) Wang, L.; Chen, Y.; Chen, S.; Long, L.; Bu, Y.; Xu, H.; Chen, B.; Krasner, S. A One-Year Long
41 Survey of Temporal Disinfection Byproducts Variations in a Consumer's Tap and Their
42 Removals by a Point-of-Use Facility. *Water Research* **2019**, *159*, 203–213.
43 <https://doi.org/10.1016/j.watres.2019.04.062>.
44
45 (104) Romera-Castillo, C.; Chen, M.; Yamashita, Y.; Jaffé, R. Fluorescence Characteristics of
46 Size-Fractionated Dissolved Organic Matter: Implications for a Molecular Assembly Based
47 Structure? *Water Research* **2014**, *55*, 40–51.
48 <https://doi.org/10.1016/j.watres.2014.02.017>.
49
50 (105) Hansen, A. M.; Kraus, T. E. C.; Pellerin, B. A.; Fleck, J. A.; Downing, B. D.; Bergamaschi, B.
51 A. Optical Properties of Dissolved Organic Matter (DOM): Effects of Biological and
52 Photolytic Degradation. *Limnology and Oceanography* **2016**, *61* (3), 1015–1032.
53 <https://doi.org/10.1002/lno.10270>.
54
55 (106) Wang, J. J.; Dahlgren, R. A.; Erşan, M. S.; Karanfil, T.; Chow, A. T. Wildfire Altering
56 Terrestrial Precursors of Disinfection Byproducts in Forest Detritus. *Environmental*
57 *Science and Technology* **2015**, *49* (10), 5921–5929. <https://doi.org/10.1021/es505836m>.
58
59
60

- 1
2
3 (107) Jochum, L. M.; Schreiber, L.; Marshall, I. P. G.; Jørgensen, B. B.; Schramm, A.; Kjeldsen, K.
4 U. Single-Cell Genomics Reveals a Diverse Metabolic Potential of Uncultivated
5 Desulfatiglans-Related Deltaproteobacteria Widely Distributed in Marine Sediment.
6 *Frontiers in Microbiology* **2018**, *9* (SEP). <https://doi.org/10.3389/fmicb.2018.02038>.
7
8 (108) Danczak, R. E.; Johnston, M. D.; Kenah, C.; Slattery, M.; Wilkins, M. J. Capability for
9 Arsenic Mobilization in Groundwater Is Distributed across Broad Phylogenetic Lineages.
10 *PLoS ONE* **2019**, *14* (9). <https://doi.org/10.1371/journal.pone.0221694>.
11
12 (109) Abraham, B. S.; Caglayan, D.; Carrillo, N. v.; Chapman, M. C.; Hagan, C. T.; Hansen, S. T.;
13 Jeanty, R. O.; Klimczak, A. A.; Klingler, M. J.; Kutcher, T. P.; Levy, S. H.; Millard-Bruzos, A.
14 A.; Moore, T. B.; Prentice, D. J.; Prescott, M. E.; Roehm, R.; Rose, J. A.; Yin, M.; Hyodo, A.;
15 Lail, K.; Daum, C.; Clum, A.; Copeland, A.; Seshadri, R.; del Rio, T. G.; Eloë-Fadrosh, E. A.;
16 Benskin, J. B. Shotgun Metagenomic Analysis of Microbial Communities from the
17 Loxahatchee Nature Preserve in the Florida Everglades. *Environmental Microbiomes*
18 **2020**, *15* (1). <https://doi.org/10.1186/s40793-019-0352-4>.
19
20 (110) Pester, M.; Knorr, K. H.; Friedrich, M. W.; Wagner, M.; Loy, A. Sulfate-Reducing
21 Microorganisms in Wetlands - Fameless Actors in Carbon Cycling and Climate Change.
22 *Frontiers in Microbiology* **2012**, *3* (FEB). <https://doi.org/10.3389/fmicb.2012.00072>.
23
24 (111) Sáenz de Miera, L. E.; Pinto, R.; Gutierrez-Gonzalez, J. J.; Calvo, L.; Ansola, G. Wildfire
25 Effects on Diversity and Composition in Soil Bacterial Communities. *Science of the Total*
26 *Environment* **2020**, *726*. <https://doi.org/10.1016/j.scitotenv.2020.138636>.
27
28 (112) Whitman, T.; Whitman, E.; Woolet, J.; Flannigan, M. D.; Thompson, D. K.; Parisien, M. A.
29 Soil Bacterial and Fungal Response to Wildfires in the Canadian Boreal Forest across a
30 Burn Severity Gradient. *Soil Biology and Biochemistry* **2019**, *138*.
31 <https://doi.org/10.1016/j.soilbio.2019.107571>.
32
33 (113) Bowers, R. M.; Kyrpides, N. C.; Stepanauskas, R.; Harmon-Smith, M.; Doud, D.; Reddy, T.
34 B. K.; Schulz, F.; Jarett, J.; Rivers, A. R.; Eloë-Fadrosh, E. A.; Tringe, S. G.; Ivanova, N. N.;
35 Copeland, A.; Clum, A.; Becraft, E. D.; Malmstrom, R. R.; Birren, B.; Podar, M.; Bork, P.;
36 Weinstock, G. M.; Garrity, G. M.; Dodsworth, J. A.; Yooseph, S.; Sutton, G.; Glöckner, F.
37 O.; Gilbert, J. A.; Nelson, W. C.; Hallam, S. J.; Jungbluth, S. P.; Ettema, T. J. G.; Tighe, S.;
38 Konstantinidis, K. T.; Liu, W. T.; Baker, B. J.; Rattei, T.; Eisen, J. A.; Hedlund, B.; McMahon,
39 K. D.; Fierer, N.; Knight, R.; Finn, R.; Cochrane, G.; Karsch-Mizrachi, I.; Tyson, G. W.; Rinke,
40 C.; Lapidus, A.; Meyer, F.; Yilmaz, P.; Parks, D. H.; Eren, A. M.; Schriml, L.; Banfield, J. F.;
41 Hugenholtz, P.; Woyke, T. Minimum Information about a Single Amplified Genome
42 (MISAG) and a Metagenome-Assembled Genome (MIMAG) of Bacteria and Archaea.
43 *Nature Biotechnology*. Nature Publishing Group August 8, 2017, pp 725–731.
44 <https://doi.org/10.1038/nbt.3893>.
45
46 (114) Patzner, M. S.; Mueller, C. W.; Malusova, M.; Baur, M.; Nikeleit, V.; Scholten, T.;
47 Hoeschen, C.; Byrne, J. M.; Borch, T.; Kappler, A.; Bryce, C. Iron Mineral Dissolution
48 Releases Iron and Associated Organic Carbon during Permafrost Thaw. *Nature*
49 *Communications* **2020**, *11* (1). <https://doi.org/10.1038/s41467-020-20102-6>.
50
51 (115) Sharma, S.; Cavallaro, G.; Rosato, A. A Systematic Investigation of Multiheme C-Type
52 Cytochromes in Prokaryotes. *Journal of Biological Inorganic Chemistry* **2010**, *15* (4), 559–
53 571. <https://doi.org/10.1007/s00775-010-0623-4>.
54
55
56
57
58
59
60

- 1
2
3 (116) Fuchs, G.; Boll, M.; Heider, J. Microbial Degradation of Aromatic Compounds- From One
4 Strategy to Four. *Nature Reviews Microbiology* **2011**, *9* (11), 803–816.
5 <https://doi.org/10.1038/nrmicro2652>.
6
7 (117) Knicker, H.; Hilscher, A.; de la Rosa, J. M.; González-Pérez, J. A.; González-Vila, F. J.
8 Modification of Biomarkers in Pyrogenic Organic Matter during the Initial Phase of
9 Charcoal Biodegradation in Soils. *Geoderma* **2013**, *197–198*, 43–50.
10 <https://doi.org/10.1016/j.geoderma.2012.12.021>.
11
12 (118) Donhauser, J.; Niklaus, P. A.; Rousk, J.; Larose, C.; Frey, B. Temperatures beyond the
13 Community Optimum Promote the Dominance of Heat-Adapted, Fast Growing and Stress
14 Resistant Bacteria in Alpine Soils. *Soil Biology and Biochemistry* **2020**, *148*.
15 <https://doi.org/10.1016/j.soilbio.2020.107873>.
16
17 (119) Donhauser, J.; Qi, W.; Bergk-Pinto, B.; Frey, B. High Temperatures Enhance the Microbial
18 Genetic Potential to Recycle C and N from Necromass in High-Mountain Soils. *Global*
19 *Change Biology* **2021**, *27* (7), 1365–1386. <https://doi.org/10.1111/gcb.15492>.
20
21 (120) Bruns, T. D.; Chung, J. A.; Carver, A. A.; Glassman, S. I. A Simple Pyrococosm for Studying
22 Soil Microbial Response to Fire Reveals a Rapid, Massive Response by Pyronema Species.
23 *PLoS ONE* **2020**, *15* (3), 1–20. <https://doi.org/10.1371/journal.pone.0222691>.
24
25 (121) Nelson, A. R.; Sawyer, A. H.; Gabor, R. S.; Saup, C. M.; Bryant, S. R.; Harris, K. D.; Briggs,
26 M. A.; Williams, K. H.; Wilkins, M. J. Heterogeneity in Hyporheic Flow, Pore Water
27 Chemistry, and Microbial Community Composition in an Alpine Streambed. *Journal of*
28 *Geophysical Research: Biogeosciences* **2019**, *124* (11), 3465–3478.
29 <https://doi.org/10.1029/2019JG005226>.
30
31 (122) Saup, C. M.; Bryant, S. R.; Nelson, A. R.; Harris, K. D.; Sawyer, A. H.; Christensen, J. N.;
32 Tfaily, M. M.; Williams, K. H.; Wilkins, M. J. Hyporheic Zone Microbiome Assembly Is
33 Linked to Dynamic Water Mixing Patterns in Snowmelt-Dominated Headwater
34 Catchments. *Journal of Geophysical Research: Biogeosciences* **2019**, *124* (11), 3269–3280.
35 <https://doi.org/10.1029/2019JG005189>.
36
37 (123) Weber, C. F.; Lockhart, J. S.; Charaska, E.; Aho, K.; Lohse, K. A. Bacterial Composition of
38 Soils in Ponderosa Pine and Mixed Conifer Forests Exposed to Different Wildfire Burn
39 Severity. *Soil Biology and Biochemistry* **2014**, *69*, 242–250.
40 <https://doi.org/10.1016/j.soilbio.2013.11.010>.
41
42 (124) Wang, J. J.; Dahlgren, R. A.; Erşan, M. S.; Karanfil, T.; Chow, A. T. Temporal Variations of
43 Disinfection Byproduct Precursors in Wildfire Detritus. *Water Research* **2016**, *99*, 66–73.
44 <https://doi.org/10.1016/j.watres.2016.04.030>.
45
46
47
48
49
50
51
52
53
54
55
56
57
58
59
60